

**BIODIESEL PRODUCTION USING IONIC
LIQUID AS CATALYST**

LEE YEE SIN

UNIVERSITI TUNKU ABDUL RAHMAN

BIODIESEL PRODUCTION USING IONIC LIQUID AS CATALYST

LEE YEE SIN


**A project report submitted in partial fulfilment of the
requirements for the award of Bachelor of Chemical
Engineering with Honours**

**Lee Kong Chian Faculty of Engineering and Science
Universiti Tunku Abdul Rahman**

May 2023

DECLARATION

I hereby declare that this project report is based on my original work except for citations and quotations which have been duly acknowledged. I also declare that it has not been previously and concurrently submitted for any other degree or award at UTAR or other institutions.

Signature :  _____

Name : Lee Yee Sin

ID No. : 1804306

Date : 1 May 2023

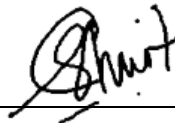
APPROVAL FOR SUBMISSION

I certify that this project report entitled “**BIODIESEL PRODUCTION USING IONIC LIQUID**” was prepared by **LEE YEE SIN** has met the required standard for submission in partial fulfilment of the requirements for the award of Bachelor of Chemical Engineering with Honours at Universiti Tunku Abdul Rahman.

Approved by,

Signature

:



Supervisor

:

Ts. Dr. Shuit Siew Hoong

Date

:

1 May 2023

Signature

:

Ng Yee Sern

Co-Supervisor

:

Dr. Ng Yee Sern

Date

:

1 May 2023

The copyright of this report belongs to the author under the terms of the copyright Act 1987 as qualified by Intellectual Property Policy of Universiti Tunku Abdul Rahman. Due acknowledgement shall always be made of the use of any material contained in, or derived from, this report.

© 2023, Lee Yee Sin. All right reserved.

ACKNOWLEDGEMENTS

I would like to thank everyone who had contributed to the successful completion of this project. I would like to express my gratitude to my research supervisor, Ts. Dr. Shuit Siew Hoong and co-supervisor Dr. Ng Yee Sern for their invaluable advice, guidance and their enormous patience throughout the development of the research.

In addition, I would also like to express my gratitude to my loving parents and friends who had helped and given me encouragement throughout the period in completing my final year project.

Lastly, I offer my best regards to all who supported me towards the completion of the final year project.

ABSTRACT

The palm oil industries produce large amounts of low-grade oil wastes, known as palm fatty acid distillate (PFAD). PFAD contains high composition of free fatty acids (FFAs) which can be used to synthesis biodiesel through esterification. The esterification of FFA is conventionally carried out using strong acid the catalyst, to produce fatty acid methyl esters (FAME), commonly known as biodiesel. This research aimed to produce biodiesel from the esterification of PFAD using an ionic liquid (IL) catalyst, specifically 1-butyl-3-methylimidazolium chloride [BMIM]Cl. The research work began by characterizing [BMIM]Cl using fourier-transform infrared spectroscopy (FTIR), ultraviolet-visible (UV-Vis), and thermogravimetric analysis (TGA). Subsequently, a parameter study of the esterification of PFAD and methanol using [BMIM]Cl as catalyst was carried out with the aid of design of experiment (DOE) coupled with response surface methodology (RSM) and central composite design (CCD) to optimize the process. The studied parameters were temperature (45 – 65 °C), catalyst dosage (2 – 6 wt%), methanol to PFAD ratio (5 – 25), and reaction time (1 – 5 h). ANOVA analysis revealed that temperature had the largest effect to the PFAD conversion, followed by catalyst dosage and reaction time. The methanol to PFAD ratio was found to have an insignificant effect on the PFAD conversion. The optimization was then performed based on the maximization of conversion of PFAD. It was observed that an optimum PFAD conversion of 40.24 % was achieved at a temperature of 60 °C, with a catalyst dosage of 5 wt% and a methanol to PFAD ratio of 19.6 in 4 hours of reaction time. It can be concluded that the esterification of PFAD using [BMIM]Cl as catalyst can be an alternative method to produce biodiesel.

TABLE OF CONTENTS

DECLARATION		i
APPROVAL FOR SUBMISSION		ii
ACKNOWLEDGEMENTS		iv
ABSTRACT		v
TABLE OF CONTENTS		vi
LIST OF TABLES		ix
LIST OF FIGURES		x
LIST OF SYMBOLS / ABBREVIATIONS		xii
CHAPTER		
1	INTRODUCTION	1
1.1	General Introduction	1
1.2	Importance of the Study	2
1.3	Problem Statement	2
1.4	Aim and Objectives	4
1.5	Scope and Limitation of the Study	4
1.6	Contribution of the Study	4
1.7	Outline of the Report	5
2	LITERATURE REVIEW	6
2.1	Introduction	6
2.2	Overview of Biodiesel	6
2.2.1	Advantages and Disadvantages of Biodiesel	7
2.2.2	Physical and Chemical Properties of Biodiesel	8
2.2.3	Biodiesel Consumption and Production in the World	10
2.3	PFAD as Feedstock for Biodiesel Production	12
2.4	Biodiesel Synthesis Method	12

	2.4.1 Esterification Reaction	13
	2.4.2 Transesterification Reaction	14
	2.4.3 Comparison Between the Synthesis Methods	15
2.5	Overview of Ionic Liquids	17
	2.5.1 Classification of Ionic Liquids	18
	2.5.2 Properties of Ionic Liquids, [BMIM]Cl	19
	2.5.3 Application of Ionic Liquid in Biodiesel Production	20
3	METHODOLOGY AND WORK PLAN	23
	3.1 Introduction	23
	3.2 Apparatus and Instruments	24
	3.3 Characterization of 1-Butyl-3-Methylimidazolium Chloride [BMIM]Cl	26
	3.3.1 FTIR	26
	3.3.2 UV-Vis	26
	3.3.3 TGA	26
	3.4 Reactor System for Esterification of PFAD using [BMIM]Cl as Catalyst	27
	3.5 Parameter Study	28
	3.5.1 Characterization of Biodiesel Sample	29
	3.5.2 Conversion of PFAD	29
	3.6 Statistical Analysis and Optimization using Design of Experiments (DOE)	30
4	RESULTS AND DISCUSSION	32
	4.1 Introduction	32
	4.2 Characterization of 1-Butyl-3-Methylimidazolium Chloride Ionic Liquid	32
	4.2.1 FTIR Analysis	32
	4.2.2 UV-Vis Analysis	34
	4.2.3 TGA Analysis	35
	4.3 Parameter Study for the Esterification of Palm Fatty Acid Distillate Using 1-Butyl-3- Methylimidazolium as Catalyst	35

4.3.1	Design of Experiment (DOE)	36
4.3.2	Statistical Analysis of Results	37
4.3.3	Development of Regression Model Equation	39
4.3.4	Effect of Process Parameters on Esterification of Palm Fatty Acid Distillate Using 1-Butyl-3-Methylimidazolium as Catalyst	40
4.4	GC Analysis	46
	Retention time (min)	46
	Type of FFAs	46
	Retention time (min)	46
	Type of Methyl Ester	46
4.5	Process Optimization Studies	49
4.6	Summary	50
5	CONCLUSIONS AND RECOMMENDATIONS	51
5.1	Conclusions	51
5.2	Recommendations for future work	52
	REFERENCES	53
	APPENDICES	59

LIST OF TABLES

Table 2.1:	Physical and Chemical Properties of Biodiesel.	9
Table 2.2:	Advantages and Disadvantages of Esterification and Transesterification Reaction.	16
Table 2.3:	Properties of [BMIM][Cl] via UNIFAC Method.	19
Table 2.4:	Review of Reaction Conditions Found in Literature.	22
Table 3.1:	List of Chemicals and Specifications Used in This Study.	24
Table 3.2:	List of Instruments and Functions.	25
Table 3.3:	Range of Reaction Condition for Esterification Reaction.	28
Table 3.4:	Coded and Actual Values of Process Parameters.	30
Table 3.5:	Design Matrix of Experiments.	31
Table 4.1:	Various Combinations of Process Parameter and Conversion.	36
Table 4.2:	ANOVA result of Response Surface Model for Esterification of PFAD using [BMIM]Cl as Catalyst.	38
Table 4.3:	Identification of Peaks in GC Spectrum of Pure PFAD.	46
Table 4.4:	Identification of Peaks in GC Spectrum of Biodiesel Sample.	46
Table 4.5:	Constraints for Optimization of PFAD Conversion.	49
Table 4.6:	Model Validation Conducted at Optimum Condition.	50

LIST OF FIGURES

Figure 2.1:	Renewable Energy for Transport in EU.	11
Figure 2.2:	Global Biofuel Production from 2000 to 2021.	11
Figure 2.3:	The General Chemical Reaction of Esterification Reaction.	13
Figure 2.4:	Mechanism Scheme of Acid-catalysed Esterification Reaction.	14
Figure 2.5:	The General Chemical Reaction of Transesterification Reaction.	15
Figure 2.6:	The Mechanism Scheme for Acid-catalysed Transesterification.	15
Figure 2.7:	Common Cation and Anion in Ionic Liquids.	18
Figure 2.8:	Structural Formula of [BMIM]Cl.	20
Figure 3.1:	Schematic Diagram for Overall Research Methodology.	23
Figure 3.2:	Schematic Diagram of the Reactor System for Esterification Reaction of PFAD.	27
Figure 4.1:	FTIR Spectra of [BMIM]Cl.	33
Figure 4.2:	UV-Vis Spectrum of [BMIM]Cl.	34
Figure 4.3:	TGA Curve for [BMIM]Cl.	35
Figure 4.4:	Graph of Predicted versus Actual Values of PFAD Conversion ($R^2=0.9483$).	40
Figure 4.5:	Effect of temperature to conversion of PFAD (catalyst dosage = 4 wt%, methanol to PFAD ratio = 15, reaction time = 3 h).	42
Figure 4.6:	Effect of catalyst dosage to conversion of PFAD (temperature = 55 °C, methanol to PFAD ratio = 15, reaction time = 3 h).	43
Figure 4.7:	Effect of to methanol to PFAD ratio conversion of PFAD (temperature = 55 °C, catalyst dosage = 4 wt%, reaction time = 3h).	44

- Figure 4.8: Effect of reaction time to conversion of PFAD (temperature = 55 °C, catalyst dosage = 4 wt%, methanol to PFAD ratio = 3h). 45
- Figure 4.9: GC Spectrum of Pure PFAD. 47
- Figure 4.10: GC Spectrum of Biodiesel Sample (temperature = 65 °C, catalyst dosage = 4 wt%, methanol to PFAD ratio = 10, reaction time = 4h). 48

LIST OF SYMBOLS / ABBREVIATIONS

n	number of mole
P_c	critical pressure, bar
T_b	boiling temperature, °C
T_c	critical temperature, °C
X	conversion, %
x	molar ratio
ρ	density, g/cm ³
AILs	acidic ionic liquids
BAILs	Brønsted acidic ionic liquids
BILs	basic ionic liquids
BLAILs	Brønsted-Lewis acidic ionic
FAME	fatty acid methyl ester
FFAs	free fatty acids
FIC	flame ionization detector
FTIR	Fourier transform infrared spectroscopy
GC	gas chromatography
GHGs	greenhouse gases
ILs	ionic liquids
LAILs	Lewis acidic ionic liquids
PFAD	palm fatty acid distillate
RSM	response surface methodology
TGA	thermogravimetric analysis
UV	ultraviolet
Vis	visible
VOCs	volatile components
WCO	waste cooking oil
Al^{3+}	aluminium ions with three positive charges
$AlCl_3$	aluminium (III) chloride
[AMIM]Br	1-allyl-3-methylimidazolium bromide
[BMIM]CH ₃ SO ₃	1-butyl-3-methylimidazolium tosylate

[BMIM]Cl	1-butyl-3-methylimidazolium chloride
[BMIM]Cl-FeCl ₃	functionalized 1-butyl-3-methylimidazolium chloride with iron (III) chloride ionic liquid
[BSMBIM]CF ₃ SO ₃	3-methyl-1-(4-sulfo-butyl)-benzimidazolium trifluoromethanesulfonate
[BMIM]HSO ₄	1-butyl-3-methylimidazolium hydrogen sulfate
C	carbon
CO ₂	carbon dioxide
Co ²⁺	cobalt ions with two positive charges
CoCl ₂	cobalt (II) chloride
Cu ²⁺	copper ions with two positive charges
EAN	ethylammonium nitrate
[EMIM]Br	1-ethyl-3-methylimidazolium bromide
Fe ³⁺	iron ions with three positive charges
FeCl ₃	iron (III) chloride
HCl	hydrochloric acid
[HMIM]HSO ₄	1-methylimidazolium hydrogen sulfate
H ₂ SO ₄	sulfuric acid
KBr	potassium bromide
KOH	potassium hydroxide
Li ⁺	lithium ions
Mn ²⁺	manganese ions with two positive charges
NaOH	sodium hydroxide
NO _x	nitrogen oxide
SO _x	sulfur oxide
Zn ²⁺	zinc ions with two positive charges
ZnCl ₂	zinc (II) chloride

CHAPTER 1

INTRODUCTION

1.1 General Introduction

Energy is crucial for developing a country and its economy as all human activities rely on supply of energy. Furthermore, the demand for energy is increasing with the growth of population (Owusu and Asumadu-Sarkodie, 2016). According to Gholami, Pourfayaz and Maleki (2020), oil is one of the major sources of global energy consumption and sustainable development has become a pressing issue for governments and organizations. The use of fossil fuels has speed up the transformation of the entire energy system due to its environmental concerns (Harjanne and Korhonen, 2019).

Renewable energy technology is the only way to mitigate climate change without affecting the supply of energy. Renewable energy is derived from natural sources which can constantly replenish themselves without depletion (Owusu and Asumadu-Sarkodie, 2016). The most common types of renewable energy sources are biofuels, hydropower, nuclear, solar, wind, geothermal, and ocean. In 2019, around 9.4% of the world's total energy was supplied by biofuels (International Energy Agency, 2021). Biofuel can also be known as bio-based fuels, which are obtained from biological sources or biomass.

One of the most common types of biofuels is biodiesel which is an alkyl ester of long-chain fatty acids, C14-C24 (Panchal, et al., 2022). Biodiesel can be synthesized from renewable lipid feedstocks through either transesterification or esterification reactions. The transesterification reaction is performed using triglycerides as the reactant while the esterification reaction is using free fatty acids (FFAs). Both reactions are conducted using alcohol in the presence of catalysts. The most used catalysts in biodiesel production included acid catalysts, alkaline catalysts, and ionic liquids (ILs). Ionic liquids are type of Newtonian liquid that consists of cations and anions (Ong, et al., 2021). Ionic liquids have been involved in recent research for esterification and transesterification reactions due to their low environmental impact and high separation efficiency.

1.2 Importance of the Study

This study determined the effectiveness of ionic liquids in esterification of PFAD to produce biodiesel. The application of esterification reaction in producing biodiesel has been studied extensively by research. However, limited attention has been given to the utilization of ionic liquid as a catalyst for the esterification of PFAD. The results of this study can serve as served as a reference point for the future research to enhance the biodiesel synthesis process.

1.3 Problem Statement

The non-renewability of fossil fuels and the threat of global warming due to climate change has accelerated the need for alternative energy sources. The rapidly growing demand for energy has caused the increased consumption of fossil fuels. Fossil fuels, particularly petroleum oil, have historically been the major energy source since the mid-20th century. In the year of 2019, oil is the world's most used energy source, which accounts for 40.4% of the world's total final consumption (International Energy Agency, 2021). However, the combustion of fossil fuels to generate heat and electricity is the major contributor to carbon dioxide (CO₂) emission (Latchubugata, et al., 2018). CO₂ is a type of greenhouse gases (GHGs) that contributes to climate change and global warming. Moreover, the limited availability of fossil fuels has made them increasingly expensive.

As a renewable energy source, biodiesel has been proposed as a partial or complete substitute for diesel. Biodiesel is more environmental friendly than fossil fuels, emitting net zero net CO₂, low sulfur oxide (SO_x), and produced from renewable biological sources (Ullah, et al., 2017). Additionally, biodiesel is safer than diesel as it has a higher flash point as stated by Gouveia et al. (2017), with the flash point of biodiesel and conventional diesel being 150 °C and 55 °C to 60 °C respectively. Therefore, biodiesel has the potential to replace fossil fuels.

However, the conventional homogeneous acid and base catalysts employed in biodiesel production have several drawbacks. These catalysts, such as NaOH and H₂SO₄, are corrosive, non-environmental friendly, and have low reusability, leading to lower biodiesel yield (Ullah, et al., 2017). Moreover, the use of a homogeneous base catalyst for transesterification can lead to

saponification and emulsification processes, leading to lower yield of biodiesel (Ullah, et al., 2017). This is caused by the presence of high FFAs and moisture content in raw materials. The reaction between water, FFAs, and base catalysts form a gel-like mixture that poses separation and purification problems, resulting in higher purification costs (Panchal, et al., 2022).

Furthermore, the presence of water in the feedstock will hydrolyse triglyceride to FFAs and diglyceride, causing low biodiesel yield. Similarly, water content in the raw materials can hydrolyse the obtained biodiesel back to FFAs (Ullah, et al., 2018). Homogeneous acid catalysts can solve the saponification problem, but they require higher operating temperature and pressure and longer reaction time, as well as higher amount of alcohol, to achieve higher biodiesel conversion rates (Gholami, et al., 2020). Some attempts have been made to minimize the disadvantage of homogeneous acid and base catalysts. Latchubugata, et al. (2018) stated that the heterogeneous catalysts are more environmental friendly than homogeneous catalysts as the catalyst separation can be easily performed, and they can also be reused. However, the heterogeneous catalyst requires long reaction times and can become deactivated (Liu et al., 2012).

To address this issues, ionic liquids have been considered as an alternative catalyst for biodiesel synthesis reactions. Ionic liquids have unique yet advantageous properties such as non-flammability, negligible vapour pressure, recyclability, non-volatile, a wide liquid temperature, thermal stability, and excellent dissolving capacity (Ong, et al., 2021). Apart from that, the chemical structures of ionic liquids are adjustable to meet the specific application (Gholami, et al., 2020). Ionic liquids are also more environmental friendly than conventional acid and base catalysts, producing high purity of products and eases the purification process. Therefore, an alternative approach to overcome the drawbacks of existing biodiesel synthesis method is to substitute conventional catalyst with ionic liquids.

1.4 Aim and Objectives

The aim of this research was to study the biodiesel production using ionic liquids as catalyst. The following list showed the objective of the study:

1. To characterize the 1-butyl-3-methyl imidazolium chloride, [BMIM]Cl.
2. To investigate the effect of the process parameters to the esterification reaction of PFAD using [BMIM]Cl as catalyst.
3. To optimize the process parameters for the esterification reaction of PFAD using response surface methodology (RSM) coupled with central composite design (CCD).

1.5 Scope and Limitation of the Study

1-butyl-3-methyl imidazolium chloride [BMIM]Cl was chosen as the ionic liquid catalyst for biodiesel synthesis. The characterization of [BMIM]Cl was done by three analytical techniques, which were fourier transform infrared spectroscopy (FTIR), ultraviolet-visible (UV-Vis) spectrophotometer, and thermogravimetric analysis (TGA).

In order to investigate the relationship between process parameters and the conversion of PFAD, a total of 30 experiments were conducted using conditions generated by Design-Expert software. The process parameters that were varied include temperature, catalyst dosage, methanol to PFAD ratio, and reaction time. Response surface methodology (RSM) coupled with central composite design (CCD) was used to optimize the conversion rate. The conversion of PFAD was determined by measuring the acid value (AV) of the sample using titration method. Gas chromatography (GC) was employed to analyze the presence of fatty acid methyl esters (FAMES) in the biodiesel sample.

1.6 Contribution of the Study

The analysis conducted on [BMIM]Cl for its characterization can serve as a basis for future research on ionic liquids. Furthermore, the results and process parameters evaluated in this study can be utilized as a reference for enhancing the esterification of PFAD by employing [BMIM]Cl as a catalyst in future research.

1.7 Outline of the Report

The report consisted of five main chapters and the overall outline of report were presented as follows:

- i. Chapter 1: Introduction
Overview on the purpose of the report, which included brief introduction of the topic, importance of the study, problem statements, aims and objective, scope and limitation, and contribution of the study.
- ii. Chapter 2: Literature Review
The basic principle and knowledge to the topic, which included overview of biodiesel, biodiesel production method, and overview of ionic liquids.
- iii. Chapter 3: Methodology and Workplan
The methodology for conducting experiments and optimizations, as well as the necessary chemicals and equipment.
- iv. Chapter 4: Results and Discussion
The effects of various process parameters on the conversion of PFAD were investigated and discussed based on the experimental results.
- v. Chapter 5: Conclusion and Recommendations
The conclusion of the research study and recommendations to undertake.

CHAPTER 2

LITERATURE REVIEW

2.1 Introduction

A preliminary background study was conducted to gain a better understanding on the synthesis method for biodiesel production. The driving force of the literature review was to identify the research gap in current approaches for biodiesel production by reviewing the overview of biodiesel, feedstocks for biodiesel production, biodiesel synthesis method, and overview of ionic liquids.

2.2 Overview of Biodiesel

Biodiesel is a type of fuel composed of a mixture of Fatty Acid Methyl Esters (FAME), which produced by reacting alcohol with vegetable oils or animal fats (Demirbas, 2007). Biodiesel is an alternative to petrodiesel and can be applied as an additive to petroleum diesel by blending in any proportion of biodiesel with petroleum diesel. This can effectively reduce the production of greenhouse gases (GHGs) emissions such as CO₂. According to Demirbas (2007), B5 and B20 are the most common used biodiesel blend. B5 refers to up to 5% of biodiesel blends with petroleum diesel while B20 refers to 6 % to 20 % of biodiesel. They can be consumed as a transportation fuel for diesel vehicles without performing engine modification. Besides, B100 or pure biodiesel can also be used for diesel vehicles. However, B100 and high-level blends are less commonly used in the transportation sector as compared to B20 and low-level blends. This is due to its solvent effect and less energy content (Suthisripok and Semsamran, 2018). Pure biodiesel will release deposits, accumulate in the fuel tanks, and cause blockage to the fuel filter. Hence, pure biodiesel is usually used as a blend stock to produce low-level biodiesel blends.

2.2.1 Advantages and Disadvantages of Biodiesel

There are several reasons why biodiesel is chosen to replace conventional fuels. One of the reasons is due to its availability and renewability. Biodiesel is an alternative fuel that has been developed to substitute the traditional petroleum-based fuels. Biodiesel is a renewable energy source since the raw materials can be replenished. Biodiesel is less hazardous than petroleum fuel due to its high flash point and biodegradability. Hence, biodiesel has a lower risk of handling, transporting, and storing than petroleum diesel (Demirbas, 2007). It can be mixed in any concentration with petroleum fuel and run-on unmodified engines.

Besides, the combustion efficiency of biodiesel is higher than petroleum fuel, as it contains oxygen, which enhances the combustion efficiency and reduces oxidation potential. In addition, biodiesel has lubricant properties that can prolong the lifespan of the engine. Furthermore, biodiesel has the advantage of low emission. Combustion of biodiesel rather than petroleum diesel can also reduce the emission of carbon monoxide and harmful particulates. Fukuda, Kondo and Noda (2001) stated that pure biodiesel fuel can decrease CO₂ emission by 78.45 % compared to petroleum diesel fuels, while B20 can lower CO₂ emission by 15.66 %. Biodiesel can also provide a reduction in SO₂ emission as it has less sulfur content as compared to petrodiesel. Based on Demirbas (2007), the sulfur content of petroleum diesel is more than biodiesel around 20-50 times.

Moreover, the biodegradability of biodiesel is higher than petrodiesel. According to the research conducted by Zhang, et al. (1998), biodiesel degrades four times faster than petroleum diesel. The results show that biodiesel was 77-89 % biodegraded after 28 days, while diesel was only about 18%. This is due to the pure fatty acids in biodiesel, which are hydrocarbon chains in ester form with two oxygen atoms attached at one end. This chemical structure makes them very biologically active since they can be recognized and degraded immediately by enzymes (Zhang, et al., 1998). Meanwhile, diesel fuels consist of hydrocarbon chains in alkanes form and no oxygen attached to the end. Thus, diesel fuels are less biologically active and rely on strong adaptability microorganisms which produce enzymes that can recognize the molecules (Mariano et al., 2009)

However, biodiesel produces higher nitrogen oxide (NO_x) emissions compared to diesel fuels when used in diesel engines. NO_x contributes to the ozone and acid rain formation. Besides, biodiesel has some drawbacks, including lower energy content, higher cloud and pour point, and higher viscosity than conventional diesel. Higher viscosity will increase the difficulty of the fuel pumping. In addition, biodiesel has operating disadvantages such as cold start issues, injector coking, lower engine power, and higher copper strip corrosion (Demirbas, 2007). This will increase the biodiesel fuel consumption and the overall cost.

2.2.2 Physical and Chemical Properties of Biodiesel

Biodiesel is a liquid fuel with colour ranges from yellow to dark brown. The properties of biodiesels are varied by the types of oils. Hence, the physical and chemical properties of biodiesels that are derived from different raw materials were collected to define the range of the properties and to compare with petroleum-based diesel as shown in Table 2.1. The kinematic viscosity is a crucial property as it affects the fuel spray pattern and the cold start problem. Besides, higher viscosity of fuel produces larger droplet sizes. This will cause problems such as improper air-fuel mixing, high emission of particulates, and poor combustion. Lower viscosity is required to achieve a better injection operation. Table 2.1 showed that the viscosity of biodiesel is 3.6 to 5.39 mm^2/s while diesel fuel is 3.5 to 12 mm^2/s . It showed that biodiesel is viable to replace petroleum diesel.

Based on Sani, et al. (2018), flash point is one of the important properties when accessing the flammability hazard of the material. Flash point of a substance is the temperature at which it can ignite when exposed to an ignition source such as flame or spark. From Table 2.1, biodiesel has a lower flash point than conventional fuel. Therefore, biodiesel has high volatility properties, and it is safer than conventional diesel during transportation and storage. Moreover, the cetane number is used to determine the ignition quality of fuels. The molecular structure of fatty acids and their carbon chain length can affect the cetane number of a fuel (Sani, et al., 2018). A high cetane number reduces the rate of injection and ignition delay. From Table 2.1, biodiesel contains high cetane number than diesel fuel due to its high oxygen content.

Table 2.1: Physical and Chemical Properties of Biodiesel.

Oil	Density (kg/m ³)	Kinematic viscosity (mm ² /s)	LHV (MJ/kg)	Flash points (°C)	Acidity (mg KOH/g)	Cetane number	Sulfur content (wt %)	Reference
Watermelon seed	885.3 ^a	5.35 ^b	45	147.5	-	44.47	0.13	(Martins, et al., 2015; Sani, et al., 2018)
Fish	867 ^c	3.58 ^b	38.5	147	0.19	-	-	(Martins, et al., 2015 ; Anguebes-Franceschi, et al., 2019)
Jatropha	890 ^a	3.8 ^b	40.9	87	0.2	51.6	-	(Ita, et al., 2018; Ong, et al., 2021)
Sunflower	860 ^a	4.6 ^d	33.5	178.1	0.032	49	0.04	(Fukuda, Kondo and Noda, 2001; Santos, et al., 2011)
Soybean	850 ^a	4.2 ^b	33.5	178	0.30	45	0.035	(Fukuda, Kondo and Noda, 2001)
Peanut	885 ^a	4.9 ^d	33.6	176	-	54	-	(Fukuda, Kondo and Noda, 2001)
Babassu	870 ^e	3.6 ^d	31.8	127	0.39	63	-	(Fukuda, Kondo and Noda, 2001; Figueredo, et al., 2020)
Diesel Fuel	830 - 840 ^c	3.50-12 ^b	35.5	59	-	51	0.175	(Fukuda, Kondo and Noda, 2001; Sagat and Toncu, 2015; Sani, et al., 2018;)

^a at 29 °C ; ^b at 40 °C; ^c at 15 °C; ^d at 37.8 °C; ^e at 20 °C; **LHV**: lower heating value

2.2.3 Biodiesel Consumption and Production in the World

Global biofuel consumption and production have gradually increased since the early 2000s. The share of total biofuel production has rapidly increased from 3.3 % to about 32 % from the year 2000 to 2020, which is nearly 10-fold (Enerdata, 2021). Europe and Asia were the world's largest producers and consumers of biodiesel in 2019. The biodiesel produced from Europe accounted for 33 % of global production in 2019 while Asia produced 27 % of the world's biodiesel production in 2019. Besides, Europe and Asia were the main consumers of biodiesel in 2019 as well (Enerdata, 2021).

According to Renewable Energy Progress Report (2020), the total consumption of biofuels in Europe was about 16 597 ktoe in 2018. Biodiesel constituted the most biofuels consumed in Europe, which is 77 %. Indonesia (17 %) and Malaysia (9 %) were the main countries that exported palm oil to Europe. In the European Union (EU), biodiesel was the primary renewable energy source, which is 77 %. Indonesia (17 %) and Malaysia (9 %) were the main countries that exported palm oil to Europe. The transportation sector in EU heavily relies on biofuels as the primary source of renewable energy. As reported in the Renewable Energy Progress Report (2017), biodiesel accounts for 79 % of the biofuels used in the transportation section in 2015, which makes up 88 % of the total renewable energy used in this sector. Figure 2.1 presented the amount of renewable energy employed in the transportation sector in the EU in 2015.

Enerdata (2021) stated that the United States (US) was identified as the largest biofuels producer in the world, which produced 2 432 trillion Btu of biofuel in 2019. Based on the statistic from (U.S. Energy Information Administration (EIA), 2022), there were 220 trillion Btu of biofuel production comes from biodiesel. However, biofuel production in the US encountered its first reduction in 2020, returning to the 2014 production level. The production reduced by nearly 10 % from 2 432 trillion Btu in 2019 to 2 194 trillion Btu in 2020. In addition, the growth of global biofuel production has also observed a sharp decline in 2020. The global biofuel production decreased by 11.6 % which was about 146 billion litres. This was due to pandemic restrictions and border restrictions resulting from COVID-19. The global biofuel production from 2000

to 2021 can be observed in Figure 2.2. Moreover, some countries have delayed their policy implementation due to the COVID-19 pandemic, and this had also impacted the biofuel consumption. Despite facing challenges of the pandemic, rising production prices and delayed policy implementation, the global biofuel demand in 2021 had a positive growth (IEA, 2019). The annual global biofuel demand was also forecasted to increase by 28% and reach 186 billion litres by 2026 (IEA, 2019).

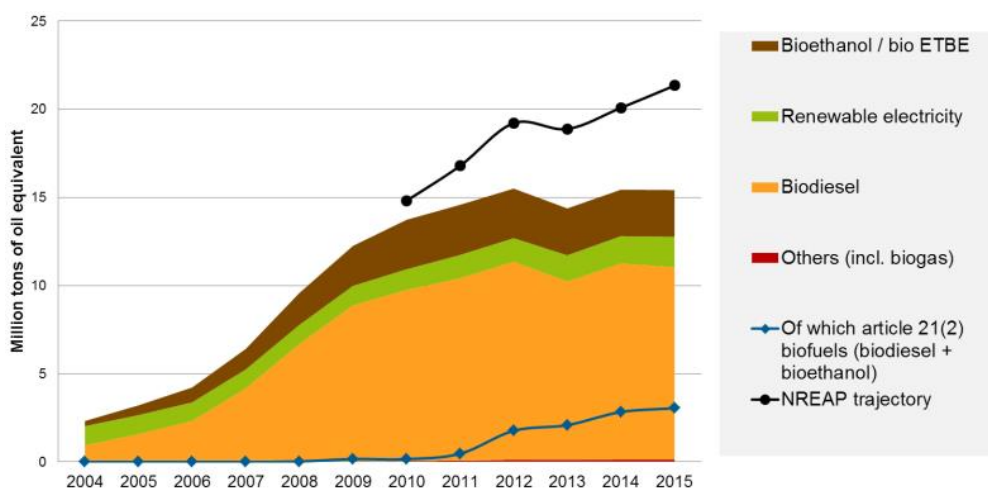


Figure 2.1: Renewable Energy for Transport in EU (Renewable Energy Progress Report, 2017).

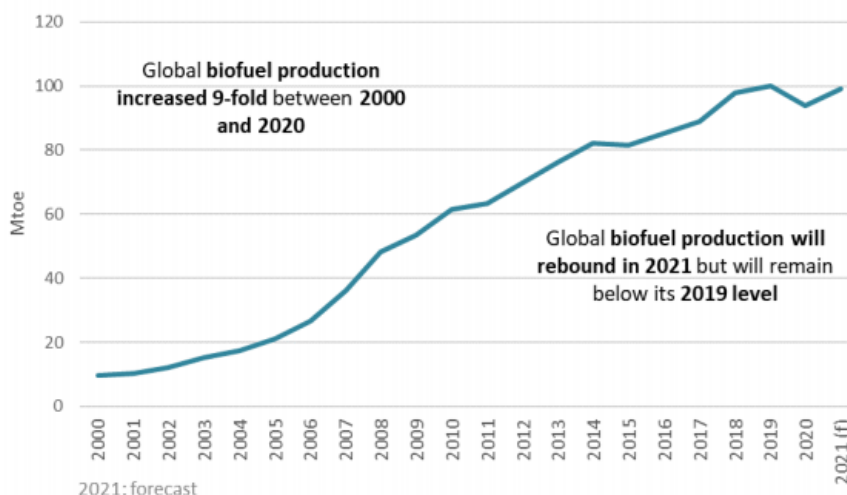


Figure 2.2: Global Biofuel Production from 2000 to 2021 (Enerdata, 2021).

2.3 PFAD as Feedstock for Biodiesel Production

Biodiesel required a higher production cost than conventional diesel. This is mainly due to the expensive feedstocks. Besides, the production of biodiesel using edible oils could cause competition with the food market and affect the food supply (Fontana, 2018). Hence, the feedstock for biodiesel production has been switch to non-edible oils to avoid interference with the food supply (Budiman, et al., 2018).

PFAD is one of the potential non-edible feedstocks for biodiesel. PFAD is a by-product from crude palm oil refining process in which the free fatty acids (FFAs) are removed from the palm fruits through distillation (Palm Fatty Acid Distillate (PFAD) in biofuels, n.d.). PFAD has lower market value than palm oil as it is non-consumable by human. Hence, it will not affect the food supply chain. The research from Shuit (2015) showed that PFAD contained high amount of FFAs which is 98 %. Therefore, PFAD could be one of the potential economical feedstocks for the synthesis of biodiesel through esterification. However, the esterification of PFAD with high FFA content, required a high excess of reactants to increase the productivity which is causing the production method is inefficient for large scale biodiesel production (Budiman, et al., 2018).

2.4 Biodiesel Synthesis Method

Esterification is one of the reaction pathways that can be employed in producing biodiesel from FFAs. The esterification reaction is usually performed using strong acid as catalyst since alkaline catalysts will react with FFAs and undergo saponification. Besides, biodiesel can also be synthesized via transesterification from vegetable oils or animal fats. This reaction can be carries using catalysts such as acid, alkaline, ionic liquids, and lipases. The case-catalysed transesterification requires a slightly higher operating temperature than acid-catalysed transesterification. Both synthesis pathways require alcohol to convert the oils to biodiesel. According to Andreani and Rocha (2012), methanol is the most employed alcohol in the synthesis of biodiesel due to its low cost and physicochemical advantages such as small molecular size. Biodiesel that obtained from methanol can be known as fatty acid methyl esters (FAMES).

2.4.1 Esterification Reaction

Esterification reaction is a chemical process of forming an ester by combining a carboxylic acid with alcohol through condensation. Esterification is a reversible reaction, and the yield can be enhanced by shifting the equilibrium towards product formation. This can be achieved through “input-pushed” or “output-pulled”. Input-pushed refers to the addition of excess reactants while output-pulled refers to products continuously removed from the reaction system (Andreani and Rocha, 2012). Figure 2.3 showed the general chemical reaction for an esterification reaction.

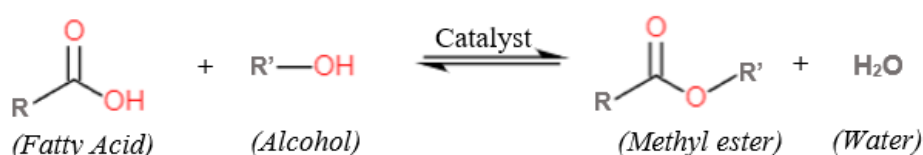


Figure 2.3: The General Chemical Reaction of Esterification Reaction (Andreani and Rocha, 2012).

The reaction mechanism for an acid-catalysed esterification reaction consists of five steps as shown in Figure 2.4. The first step (1) is the oxygen from the carbonyl group of carboxylic acid captures the hydrogen ion of acid catalyst to form protonated carbonyl substrate. In the second step (2), the protonated carbonyl substrate is attacked by the nucleophilic oxygen atom of alcohol and generates a tetrahedral intermediate. Then, the third step (3) is the proton transfer from a hydroxyl group to another hydroxyl group and obtaining a second tetrahedral intermediate. In the fourth step (4), the acyl-oxygen bond breaks and generates a protonated ester and water molecule. The last step (5) of the reaction is a proton leaves the protonated esters, producing an ester product and regenerating the acid catalyst.

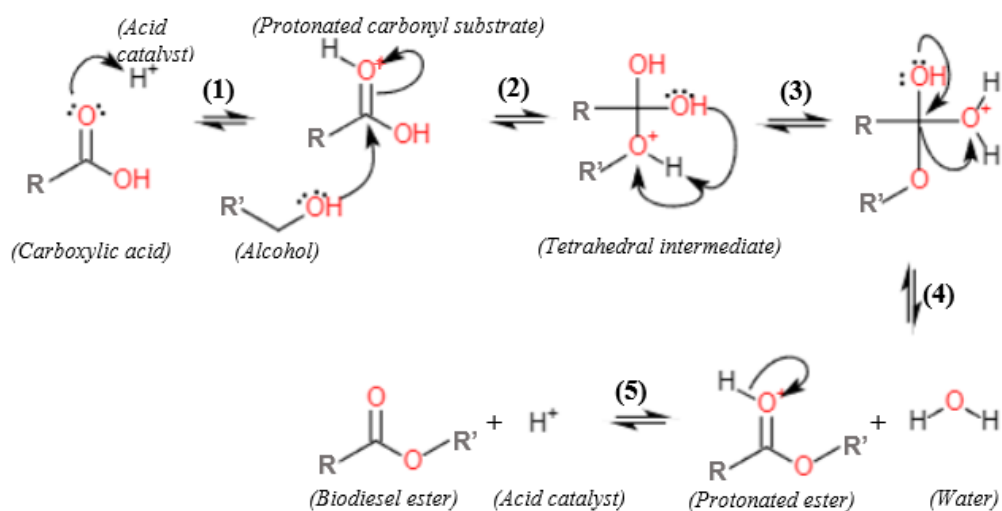


Figure 2.4: Mechanism Scheme of Acid-catalysed Esterification Reaction (Zeng, et al., 2012).

2.4.2 Transesterification Reaction

Biodiesel is usually obtained by transesterification of natural oils and fats, where alcohol is used to exchange with an ester in the presence of an acid or alkaline catalyst (Mandari and Devarai, 2022). The reaction involves one mole of triglyceride with three moles of alcohol to obtain one mole of mono-alkyl ester and one mole of glycerol, as a by-product (Tabatabaei, et al., 2019). Excess alcohol is used to drive the reaction forward. The transesterification reaction is reversible, and the equilibrium is shifted towards product formation. (Koh and Tinia, 2011). Figure 2.5 showed the acid-catalysed transesterification mechanism, which involves three steps: **(1)** the acid catalyst transfers a proton to the carbonyl carbon atom of the triglyceride to produce a strong electrophile, **(2)** the electrophile reacts with alcohol and generates a tetrahedral intermediate and **(3)**, the tetrahedral intermediate is converted to diglyceride, esters, and regenerates the acid catalyst.

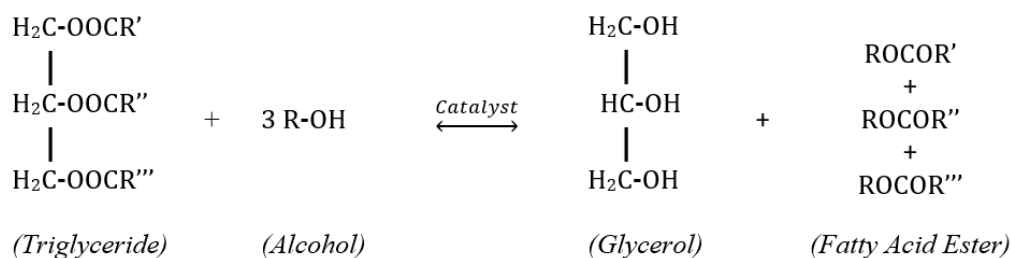


Figure 2.5 The General Chemical Reaction of Transesterification Reaction (Gebremariam and Marchetti, 2017).

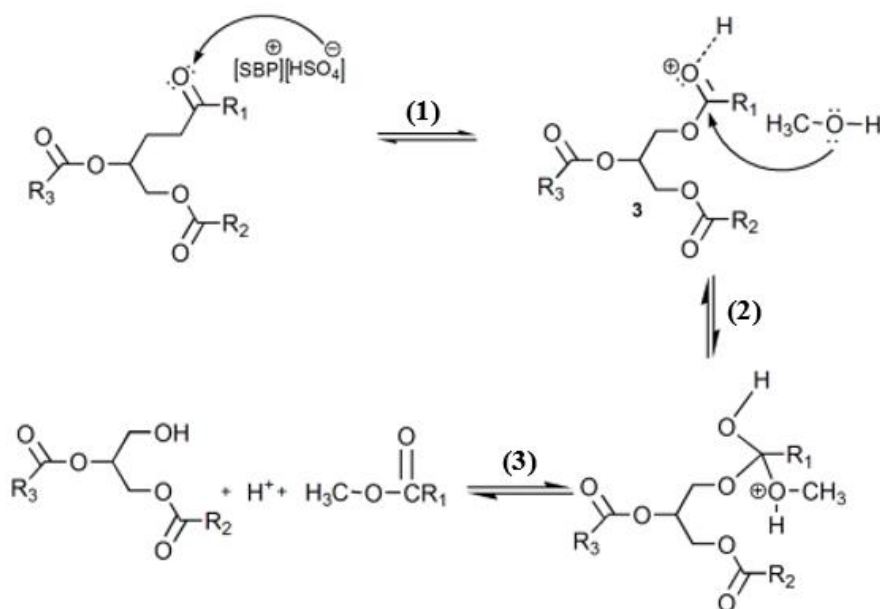


Figure 2.6: The Mechanism Scheme for Acid-catalysed Transesterification (Koh and Tinia, 2011).

2.4.3 Comparison Between the Synthesis Methods

Esterification reaction forms an ester between alcohol and fatty acid while transesterification is the reaction between triglyceride and alcohol and involves the change of R-group in ester. Moreover, esterification is mainly performed using vegetable oils as the feedstock and in the presence of an acid catalyst. Meanwhile, transesterification reaction can use either animal fats or vegetable oils by adding alcohol or acid catalyst to produce biodiesel. Esterification and transesterification reaction were compared in terms of their pros and cons as shown in Table 2.2.

Table 2.2: Advantages and Disadvantages of Esterification and Transesterification Reaction (Tabatabaei, et al., 2019; Khan, et al., 2021).

Esterification	Transesterification
<p>Advantages:</p> <ul style="list-style-type: none"> - Applicable for feedstock with high FFAs content. - It is a simple reaction process. - Reactants used and by-products produced are non-toxic to the environment. 	<p>Advantages:</p> <ul style="list-style-type: none"> - Most employed chemical pathways for biodiesel production. - Generation of valuable by-product, glycerol - Unreacted reactants (methanol) can be reused. - Mild process condition.
<p>Disadvantages:</p> <ul style="list-style-type: none"> - Slow reaction rate and low overall conversion since it is thermodynamic reversible. - Excess alcohol is needed to improve the biodiesel yield. - Strong acid catalysts which are usually used in this reaction, will cause environmental pollution. - Tertiary alcohols will carry out fast dehydration in the presence of strong acids. - Not suitable to produce phenol esters. 	<p>Disadvantages:</p> <ul style="list-style-type: none"> - Not applicable when high FFA content of the feedstock is directly used. - Dry alcohol and oil are required to prevent the formation of soap and enhance production yield. - High separation cost to separate glycerol from biodiesel, which is important to eliminate the generation of hazardous gases during combustion. - Expertise requirement. - Complex equipment requirement

2.5 Overview of Ionic Liquids

According to Lei, et al. (2017) reported that ionic liquids, which are organic salts consisting of an organic or inorganic anion and an organic cation, have been an important scientific area since Paul Walden first reported ethylammonium nitrate or ethylamine nitrate (EAN) in 1914. The chemical properties and reactivity of ionic liquids are controlled by their anion, while the physical properties, such as boiling point and density, are determined by the cation. (Gebremariam and Marchetti, 2017). In addition, the length of the R-chain of cation controls the solubility of ionic liquids in a polar fluid (Andreani and Rocha, 2012). Therefore, the properties of ionic liquids can be easily modified according to their specific application, by changing the combination of anions and cations, and the length of the R-chain. The commonly used cation and anion in ionic liquids are shown in Figure 2.7.

Ionic liquids that are usually applied in the industry are phosphorous-containing such as alkylphosphonium, and nitrogen-containing such as N-alkylpyridinium, N,N'-dialkylimidazolium, and alkylammonium (Troter, et al., 2016). The melting point of ionic liquids is below 100 °C and is present in liquid form at ambient temperature due to their large molecular size and presence of a delocalized charge, causing difficulty in packing. However, the ion attraction is enough for them to have an almost negligible vapour pressure (Andreani and Rocha, 2012). Thus, there is no VOC emission when using ionic liquids. One of the advantages of ionic liquids is that there are over 1 000 000 binary ionic liquids, and 10^{18} ternary ionic liquids available to be used in a reaction medium (Andreani and Rocha, 2012). Ionic liquids are insoluble in the organic phase and tend to remain in the aqueous phase. Hence, a biphasic system will form after the reaction, which top phase is biodiesel with a small amount of alcohol while the bottom phase consists of ionic liquids, water, and alcohol (Ullah, et al., 2018). The ionic liquid catalysts can be separated from final products using decantation, and they can be reused several times by rinsing with water and drying. According to Ramadhan, et al. (2015), ionic liquids can be reused up to 6-7 times of operation without affecting product yield significantly, and catalysts degradation did not occur. It is also usually used in small amounts than the conventional catalyst. Therefore, the cost per cycle ionic liquids would be

the same, or even cheaper than the conventional catalysts, although ionic liquids have a higher price than traditional catalysts.

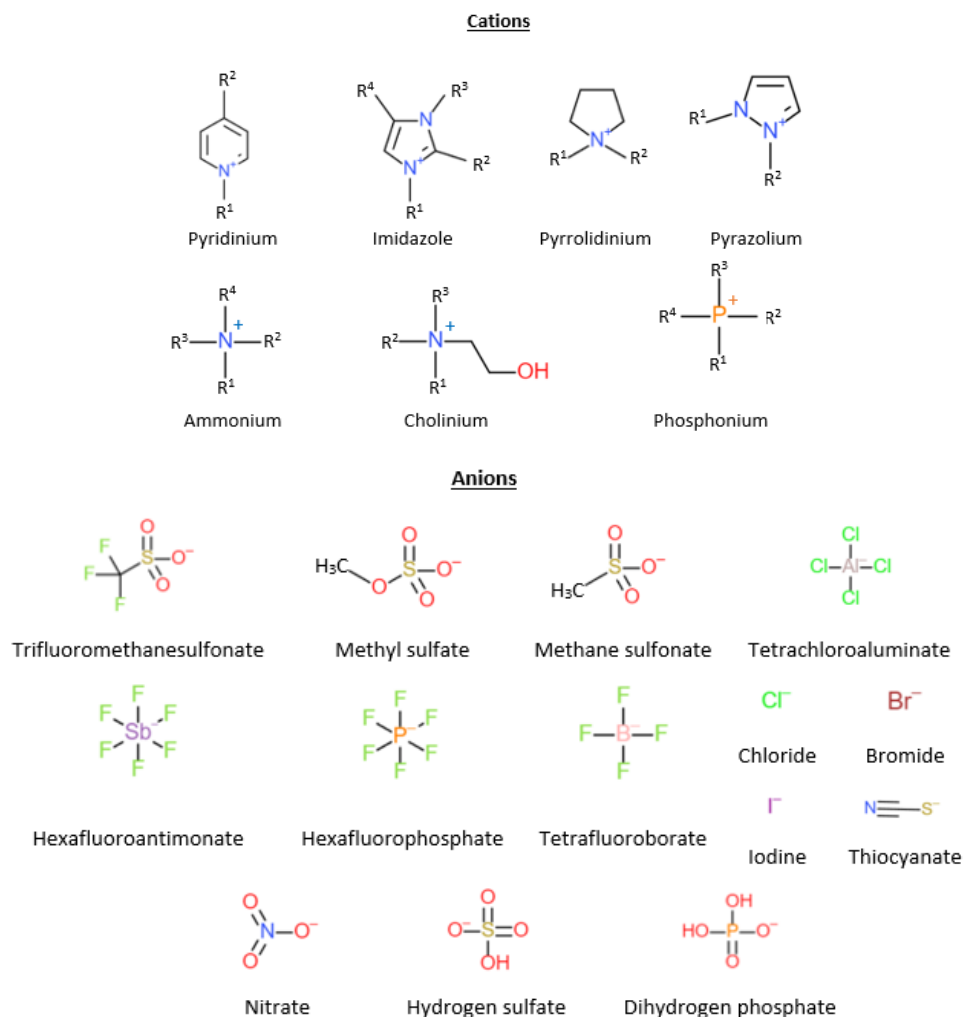


Figure 2.7: Common Cation and Anion in Ionic Liquids (Ullah, et al., 2018).

2.5.1 Classification of Ionic Liquids

Ionic liquids can be grouped into two categories, which are acidic (AILs) and basic ionic liquids (BILs) (Ong, et al., 2021). AILs and BILs have similar functions as conventional acid or alkali catalysts for biodiesel production. AILs is similar to conventional acid catalysts which can be used in both transesterification and esterification reaction, and it is suitable for raw materials with high FFAs content (Ramadhan, et al., 2015). It was reported by Ong, et al. (2021) that the AILs with a higher acidity have higher catalytic efficiency. In addition, AILs have higher catalytic efficiency at a higher temperature than BILs just like acidic catalysts. AILs can be further grouped into three types which are Brønsted acidic ionic liquids (BAILs), Lewis acidic ionic liquids

(LAILs), and Brønsted-Lewis acidic ionic liquids (BLAILs). LAILs consist of a Lewis acid site that can attract lone pair electrons from a Lewis base, whereas BAILs have one or more Brønsted acid sites that can donate a proton to a Brønsted base. BAILs such as [BMIM]CH₃CO₃, [BMIM]Cl, [AMIM]Br and [EMIM]Br, can be used in mild conditions (Guo, et al., 2011). BLAILs contain both Lewis and Brønsted acidic sites that work simultaneously to improve the catalytic efficiency (Ong, et al., 2021).

BILs are also similar to common basic catalysts which also require feedstocks with low FFAs content to avoid saponification reaction. It can only catalyse transesterification reaction just like conventional basic catalysts. Theoretically, the higher the basicity of BILs, the higher the biodiesel yield. One of the advantages of BILs over AILs is that they could be used at milder temperatures. However, AILs are more commonly used in biodiesel production compared to BILs. There are limited research studies available on the application of BILs for this purpose. BILs mainly come from imidazolium-based ILs such as imidazolid and imidazolium hydroxides (Troter, et al., 2016).

2.5.2 Properties of Ionic Liquids, [BMIM]Cl

The ionic liquid, [BMIM]Cl chosen in this research has the advantages of low toxicity, high catalytic activity, high biodegradability, high recyclability, and high liquid extraction yield (Piemonte et al., 2016). The molecular structure of [BMIM]Cl is shown in Figure 2.8. The physicochemical properties of [BMIM]Cl is poorly mentioned in the literature. Based on Piemonte *et al.* (2016), this is because of the high thermobility of ILs even at high temperatures and hence preventing reliable measurement of their boiling point. Table 2.4 showed the properties of [BMIM]Cl that are obtained by the UNIFAC method.

Table 2.3: Properties of [BMIM][Cl] via UNIFAC Method (Piemonte, et al., 2016).

Boiling temperature, T_b (°C)	Critical temperature, T_c (°C)	Critical pressure, P_c (bar)	Critical volume, V_c (cm³/mol)	Density, ρ (g/cm³, 20 °C)
284.88	515.78	27.8	568.75	1.00

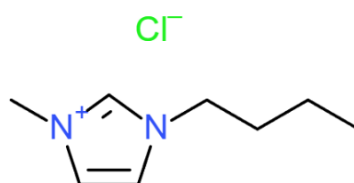


Figure 2.8: Structural Formula of [BMIM]Cl (Piemonte, et al., 2016).

2.5.3 Application of Ionic Liquid in Biodiesel Production

There are a few scientific studies published focusing on biodiesel production employing ILs as catalysts. The studies found in the literature are summarized in Table 2.4. Ullah, et al. (2017) conducted a study on biodiesel production through two steps process of esterification followed by transesterification reactions using waste cooking oils (WCOs) as raw material. The reaction was catalysed by [BSMBIM][CF₃SO₃] achieving a conversion rate of 94.52 % under the optimal conditions of a methanol to WCOs molar ratio of 12:1, temperature of 120 °C, reaction time of 4 h, and 4 wt% catalyst concentration.

Study by Roman, et al. (2019) used [HMIM]HSO₄ as the catalyst for esterification of oleic acid with methanol. Optimization on the process parameters was performed using response surface methodology (RSM), resulting in optimal process conditions of 110 °C, 8 h reaction time, 15:1 methanol to oleic acid molar ratio, and 15 wt% catalyst dosage, achieving a conversion rate of oleic acid of 95.9 %.

Yassin, et al. (2015) investigated the transesterification process of waste vegetable oils using [BMIM]Cl as the catalyst combined with FeCl₃ and AlCl₃, achieving biodiesel yields of 97% and 86%, respectively, under conditions of 8 h reaction time, 55 °C temperature, and 10:1 methanol to vegetable oil molar ratio. The research conducted by Guo, et al. (2011) used ILs with metal chlorides to produce biodiesel from un-pretreated Jatropha oil with high acid value (AV). [BMIM][CH₃SO₃]-FeCl₃ improved the reaction yield from 12% to 99.7% at optimal conditions of 120 °C, 5 h reaction time, 2:1 methanol to oleic acid molar ratio, and 3 mmol catalyst amount, while [BMIM][CH₃SO₃]-AlCl₃ enhanced the conversion rate from 44% to 98% at 80 °C.

Alimova, Ribeiro and Queiroz (2017) used [BMIM]HSO₄ to catalyse the esterification reaction of oleic acid with methanol and studied the effect of

reaction conditions such as reaction time, methanol to oil molar ratio, temperature, and catalyst dosage on methyl ester production. The optimal conditions of 10 wt% catalyst dosage, 4 h reaction time, 90 °C temperature, and 10:1 methanol/oleic acid molar ratio achieved a conversion rate of 89.7%.

Ullah, Bustam and Man (2015) also used [BMIM]HSO₄ in a two-step process involving catalytic esterification reaction of WCO with methanol and transesterification reaction with KOH. Optimal conditions for the first step were 5 wt% catalyst dosage, 15:1 methanol to WCO molar ratio, 1 h reaction time, and 160 °C temperature. Optimal conditions for the second step were 1 wt%, 1 h, and 60 °C. However, the molar ratio of KOH/WCO was not reported. Wu, et al., (2007) studied the transesterification reaction of cottonseed oil with methanol using [PySBu][HSO₄] as the catalyst. They achieved a 92% conversion rate under optimal conditions of 170 °C, reaction time of 5 h, 12:1 for methanol to oil ratio, and 0.057 for ILs/oil molar ratio.

Table 2.4: Review of Reaction Conditions Found in Literature.

Feedstock	Ionic Liquid	Rxn	Alcohol	Condition				Biodiesel yield (%)	Reference
				Molar ratio Alcohol/oil	Temp. (°C)	Reaction time (h)	Catalyst dosage (wt %)		
Waste palm cooking oil	[BSMBIM]CH ₃ SO ₃	Esterif./ Trans.	KOH	12:1	120	4	4	94.52	(Ullah, et al., 2017)
Oleic acid	[HMIM]HSO ₄	Esterif.	MeOH	14:1	110	8	15	95.9	(Roman, et al., 2019)
Vegetable oil	[BMIM]Cl-FeCl ₃	Trans.	MeOH	10:1	55	8	5g	97	(Yassin, et al., 2015)
Vegetable oil	[BMIM]Cl-AlCl ₃	Trans.	MeOH	10:1	55	8	5g	86	(Yassin, et al., 2015)
Oleic acid	[BMIM] CH ₃ SO ₃ - FeCl ₃	Esterif.	MeOH	2:1	80	5	3 mmol	99.7	(Guo, et al., 2011)
Oleic acid	[BMIM] CH ₃ SO ₃ - AlCl ₃	Esterif.	MeOH	2:1	120	5	3 mmol	98	(Guo, et al., 2011)
Oleic acid	[BMIM]HSO ₄	Esterif.	MeOH	10:1	90	4	10	89.7	(Alimova, et al., 2017)
Waste cooking oil	[BMIM]HSO ₄	Esterif./ Trans.	MeOH/ KOH	15:1	I step: 160 II step: 60	I step: 1 II step: 1	I step: 5 II step: 1	95.65	(Ullah, et al., 2015)
Cotton seed oil	1-(4-Sulfonic acid) butylpyridinium hydrogen sulfate	Trans.	MeOH	12:1	170-180	5	0.057 ^a	92	(Wu, et al., 2007)

^a molar ratio of ionic liquid to oil

CHAPTER 3

METHODOLOGY AND WORK PLAN

3.1 Introduction

The biodiesel was produced via esterification from PFAD using [BMIM]Cl as catalyst. The project started from characterization of [BMIM]Cl using FTIR, UV-Vis, and TGA. The parameter study was then conducted using the 30 sets of experimental runs generated by Design-Expert 13 software to investigate the impacts of the parameters, namely temperature, catalyst dosage, methanol to PFAD ratio, and reaction time. The PFAD conversion was determined using titration method. The optimum condition for the esterification reaction of PFAD was determined using Design Expert.

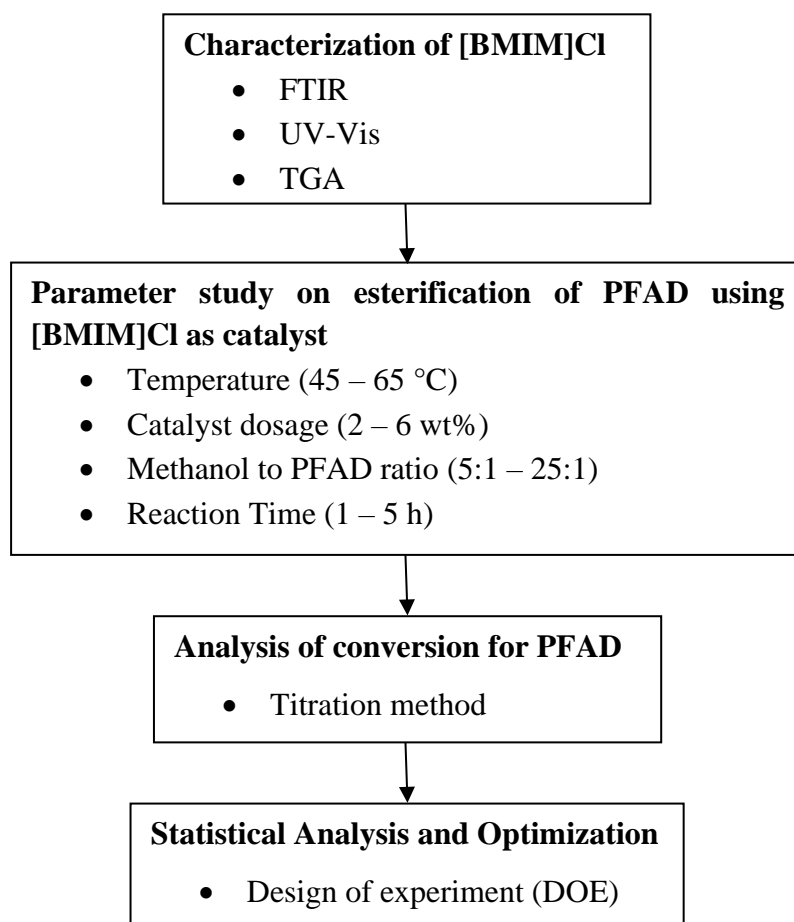


Figure 3.1: Schematic Diagram for Overall Research Methodology.

3.2 Apparatus and Instruments

Table 3.1 presented a summary of the chemical used in the experiment together with their respective specification.

Table 3.1: List of Chemicals and Specifications Used in This Study.

Chemical	Purity (%)	Supplier	Purpose of Use
Palm Fatty Acid Distillate (PFAD)	99	Refinery Palm Oil, Kuantan	To be used in the biodiesel synthesis
1-Butyl-3-Methylimidazolium Chloride ([BMIM]Cl)	≥ 98	Sigma-Aldrich, Malaysia	To be used in biodiesel synthesis
n-Hexane	95	Sigma-Aldrich, Malaysia	To be used in GC analysis
Nitrogen	99	Sigma-Aldrich, Malaysia	To provide air-free environment to reaction
Methanol	99	Fisher Scientific Malaysia	To be used in the biodiesel synthesis
Phenolphthalein	99	Kumpulan Saintifik, Malyasia	To be used in titration
Sodium Hydroxide	97	Sigma-Aldrich, Malaysia	To be used in titration
Ethanol	95	Polyscientific	To be used in titration

Table 3.2 shows the list of equipment and instruments that was used in the experiment and their purpose of use.

Table 3.2: List of Instruments and Functions.

Instrument	Function
Fourier Transform Infrared (FTIR) Spectroscopy	To identify the functional group of [BMIM]Cl
Ultraviolet-Visible (UV-Vis) spectrophotomètre	To determine the chemical structure of [BMIM]Cl
Thermogravimetric Analysis (TGA)	To determine thermal stability of [BMIM]Cl
Gas Chromatography (GC)	To identify the methyl ester content in biodiesel samples
Thermometer	To measure the temperature inside the reaction vessel
Hot plate	To supply heat to reaction system
Magnetic Stirrer Bar	To mix the chemical reactants and catalyst
3-Neck Round Bottom Flask	To act as reaction vessel
Condenser	To condense vaporize methanol
Oven	To remove excess methanol from biodiesel samples
Analytical Balance	To measure the weight of PFAD, [BMIM]Cl and biodiesel samples
Pipette	To measure and transfer solution
Burette	To measure the volume of sodium hydroxide that were used in titration

3.3 Characterization of 1-Butyl-3-Methylimidazolium Chloride [BMIM]Cl

3.3.1 FTIR

The Nicolet iS10 FTIR spectrometer supplied by Thermo Fisher Scientific was utilized to study the functional group in [BMIM]Cl. This is to ensure the ionic liquid consists of functional group of [BMIM]Cl. The FTIR spectra of [BMIM]Cl was measured in frequency range of 4000 to 400 cm^{-1} . In the characterization process, a small amount (1 – 2 drops) of [BMIM]Cl was placed on the ATR crystal for scanning. 32 scans were performed to collect the IR spectrum. Upon the completion of scanning, the sample liquid and ATR crystal were cleansed using diluted ethanol.

3.3.2 UV-Vis

UV-Vis spectrophotometer model Varian Cary 100 was used to record the UV-Vis absorption spectra of [BMIM]Cl. The UV-Vis technique was applied to ensure the ionic liquid contains the chemical structure of [BMIM]Cl by identifying the presence of an absorption band at 190 to 260 nm that was attributed to the imidazolium residue (Khalili Dermani, et al., 2019). In the sample preparation, 4 ml of [BMIM]Cl was added into a spectrophotometer glass cuvette. The absorption of the sample was measured in ultraviolet and visible light in the wavelength ranging from 200 to 800 nm.

3.3.3 TGA

The thermal stability of [BMIM]Cl was determined using a TGA model STA8000 provided by Perkin Elmer. The experiment involved adding 20 mg of the sample to the crucible, which was then heated from 30 °C to 500 °C at a heating rate of 20 °C/min under a constant nitrogen atmosphere. The TGA curve was obtained by measuring and recording the weight loss of the sample.

3.4 Reactor System for Esterification of PFAD using [BMIM]Cl as Catalyst

The process of esterification using [BMIM]Cl as catalyst was conducted in a batch reactor system which consists of a 3-neck round bottom flask with a reflux system, magnetic stirrer bar, thermometer, and heater. The 3-neck round bottom flask that were used in the experiment is a 500 mL flask with a centre socket size of 24/29 and two side socket size of 19/26. The thermometer was used to measure and monitor the temperature inside the reaction vessel. The heater used was a temperature controlled heater equipped with magnetic stirring. The temperature of reaction system was adjusted to the desired condition by controlling the temperature controller of the heater. Additionally, the reflux system consists of a condenser and cooling water was used as the cooling medium. Figure 3.2 showed the schematic diagram for the set up of batch reactor system.

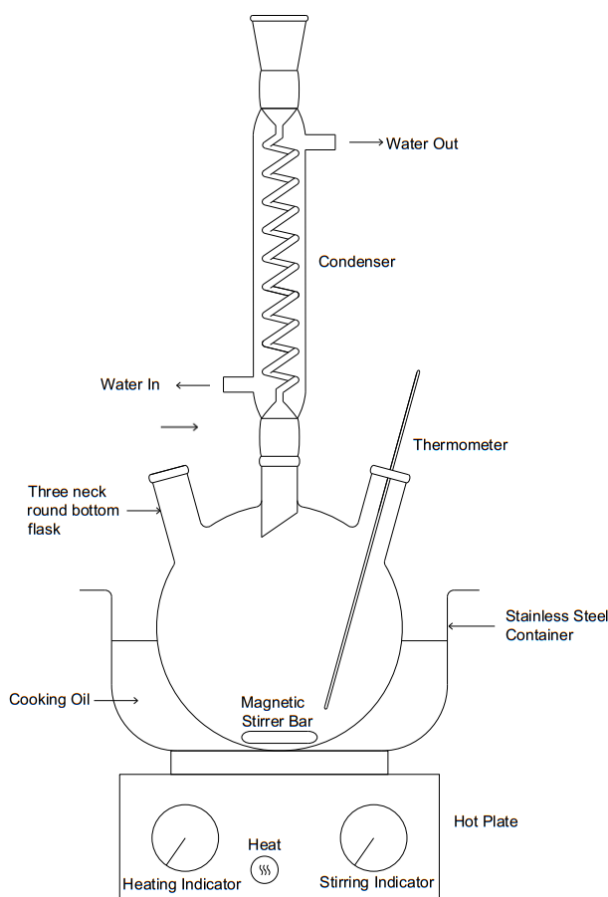


Figure 3.2: Schematic Diagram of the Reactor System for Esterification Reaction of PFAD.

3.5 Parameter Study

Table 3.3 summarized the various reaction conditions used in the esterification of PFAD using [BMIM]Cl as the catalyst to investigate the impact of parameters to the conversion rate of PFAD.

Table 3.3: Range of Reaction Condition for Esterification Reaction.

Parameters	Range
Temperature (°C)	45 – 65
Catalyst Dosage (wt%)	2 – 6
Methanol to PFAD ratio	5 – 25
Reaction Time (h)	1 – 5

The experiments were carried out with a constant stirring speed of 250 rpm. Initially, 15 g of pre-heated PFAD was added into the 3-neck round bottom flask. Then, the required volume of methanol was measured and added into the flask. A magnetic stirrer was then loaded into the flask and the glass reactor was immersed in a oil bath that placed over a heating plate. The mixture was stirred and heated to the desired temperature. Next, the pre-determined amount of [BMIM]Cl was added into the flask once the reaction temperature was achieved and stable. The reaction was then run for a desired reaction time period and the temperature was constantly monitoring throughout the reaction using a thermometer. Upon completion of reaction, the hotplate was turned off to cool down the mixture and the magnetic stirrer was removed from the flask. After the cooling process, the product mixture was then transferred from the flask to a 100 mL beaker. Next, the biodiesel mixture was placed in an oven at 80 °C for one day to evaporate the excess methanol from the product mixture. Then, the sample was stored in a 20 mL glass vial. The sample analysis and calculation of PFAD conversion was further discussed in Section 3.5.1 and Section 3.5.2.

3.5.1 Characterization of Biodiesel Sample

The gas chromatography (GC) analysis was performed using model Agilent Technologies 7890 B GC system to determine the presence of methyl ester or biodiesel in the product mixture. The GC analyser equipped with Nukol™ capillary column. The dilution factor used for the GC analysis was 40. Firstly, 0.5 mL of product sample was diluted with 9.5 mL of n-hexane. Then, 0.5 mL + 0.5 mL of diluted sample was added into a 2 mL GC vial. GC analysis was carried out using helium as the carrier gas. The initial temperature of the oven was set at 110 °C and then increased at a rate of 10 °C/min to reach a maximum temperature of 220 °C. The detection temperature and injector temperature were set at 200 °C and 220 °C, respectively.

3.5.2 Conversion of PFAD

After identified the presence of biodiesel in the sample, the conversion rate of PFAD was determined based on acid value (AV). The research conducted by Shuit (2015) showed that PFAD contains high FFA content which was about 98.46 wt% and hence the conversion of PFAD can be determined by measuring the changes of AV in the sample. According to Win and Trabold (2018), acid value can be defined as the amount of FFA content in oil requiring a computed mass of sodium hydroxide (NaOH) to neutralize it.

The AV content in the sample was determined using the titration method. Initially, the solidified sample was heated on a hotplate. Subsequently, 1 g of the biodiesel sample was placed into a 100 mL conical flask. Then, 20 mL of ethanol was added to the flask, followed by heating and stirring to ensure complete dissolution of the sample in ethanol. After that, 2-3 drops of phenolphthalein were introduced into the mixture as an indicator. The solution was then titrated with 0.1 mol/L NaOH until the solution changed from colourless to pale pink. Win and Trabold (2018) stated that the AV of sample and PFAD conversion can be determined using Equation 3.1 and Equation 3.2.

$$\text{Acid Value (AV)} \left(\frac{\text{mg NaOH}}{\text{g biodiesel}} \right) = \frac{MW_{\text{NaOH}} \times C_{\text{NaOH}} \times V_{\text{NaOH}}}{m_{\text{sample}}} \quad (3.1)$$

where,

MW_{NaOH} = Molar weight of titrant (40 g/mol)

C_{NaOH} = Concentration of titrant (mol/L)

V_{NaOH} = Volume of titrant used for titration (mL)

m_{sample} = Mass of biodiesel sample (g)

$$Conversion (\%) = \frac{AV_{PFAD} - AV_{sample}}{AV_{PFAD}} \times 100\% \quad (3.2)$$

where,

AV_{PFAD} = Acid value of PFAD (mg NaOH/g sample)

AV_{sample} = Acid value of the biodiesel sample (mg NaOH/g sample)

3.6 Statistical Analysis and Optimization using Design of Experiments (DOE)

Design-Expert Version 13 software was employed to conduct the study on the impacts of process parameters on the PFAD conversion rate. Response surface method (RSM) and central composite design (CCD) were selected as the study and design type. Table 3.4 showed the coded and actual values of process parameters that was determined based on the range of reaction condition as shown in Table 3.3. The methodology estimated 30 runs were sufficient to investigate the impact of each parameter on the response. Table 3.5 presented the design matrix of the experiment. A quadratic model was chosen to analyse the relationship between the parameters and the PFAD conversion. The process was optimized using the numerical optimization tool in the software.

Table 3.4: Coded and Actual Values of Process Parameters.

Parameters	Code	Unit	Level				
			-2 (- α)	-1	0	+1	+2 (+ α)
Temperature	A	°C	45	50	55	60	65
Catalyst dosage	B	wt%	2	3	4	5	6
Methanol to PFAD ratio	C	-	5	10	15	20	25
Reaction time	D	h	1	2	3	4	5

Table 3.5: Design Matrix of Experiments.

Run	A: Temperature (°C)	B: Catalyst dosage (wt%)	C: Methanol to PFAD ratio	D: Reaction Time (h)
1	55	4	25	3
2	55	4	15	3
3	50	5	10	4
4	55	6	15	3
5	50	5	20	2
6	50	3	10	2
7	50	3	20	4
8	55	4	15	1
9	55	4	15	5
10	55	2	15	3
11	60	5	10	2
12	50	5	10	2
13	55	4	15	3
14	65	4	15	3
15	50	3	10	4
16	55	4	15	3
17	60	3	20	2
18	60	3	10	2
19	55	4	5	3
20	55	4	15	3
21	50	3	20	2
22	60	3	20	4
23	60	5	10	4
24	60	5	20	2
25	45	4	15	3
26	55	4	15	3
27	60	5	20	4
28	60	3	10	4
29	55	4	15	3
30	50	5	20	4

CHAPTER 4

RESULTS AND DISCUSSION

4.1 Introduction

The results and discussion for this study were presented in this chapter, including the experimental work carried out. Section 4.2 discussed the characterization results of the ionic liquid, [BMIM]Cl using FTIR, UV-Vis, and TGA. Section 4.3 presented a detailed discussion on the parameter study conducted for the esterification of PFAD using [BMIM]Cl as catalyst. Furthermore, the process optimization for achieving maximum conversion of PFAD was presented in Section 4.4.

4.2 Characterization of 1-Butyl-3-Methylimidazolium Chloride Ionic Liquid

4.2.1 FTIR Analysis

Figure 4.1 showed the FTIR analysis of [BMIM]Cl with frequency ranging from 500 to 4000 cm^{-1} . The presence of aliphatic asymmetric and symmetric C-H stretch was confirmed by the peaks observed at 2958 and 2871 cm^{-1} , respectively, as reported by Kaur and Patyar (2023). Moreover, peaks ranging from 3330 to 3450 cm^{-1} were reported to be the quaternary amine salt formation with chlorine (Kassaye, et al., 2016). The peak at 3384 cm^{-1} confirmed the presence of the quaternary amine salt in the sample. Additionally, the C=N stretching was detected at 1561 cm^{-1} while C=C stretching was detected within the range of 1640 to 1680 cm^{-1} (Merck, n.d.). A strong absorption peak at around 1200 cm^{-1} was due to the presence of tertiary amine group in [BMIM]Cl (Danielewicz, et al., 2019). The -CH₃ stretching was detected at 1385 cm^{-1} (Wang, et al., 2020). According to Chemistry LibreTexts (2014), the peak at 623 cm^{-1} was the outer bending vibration of C-H. Overall, the FTIR spectra confirmed that the sample was [BMIM]Cl.

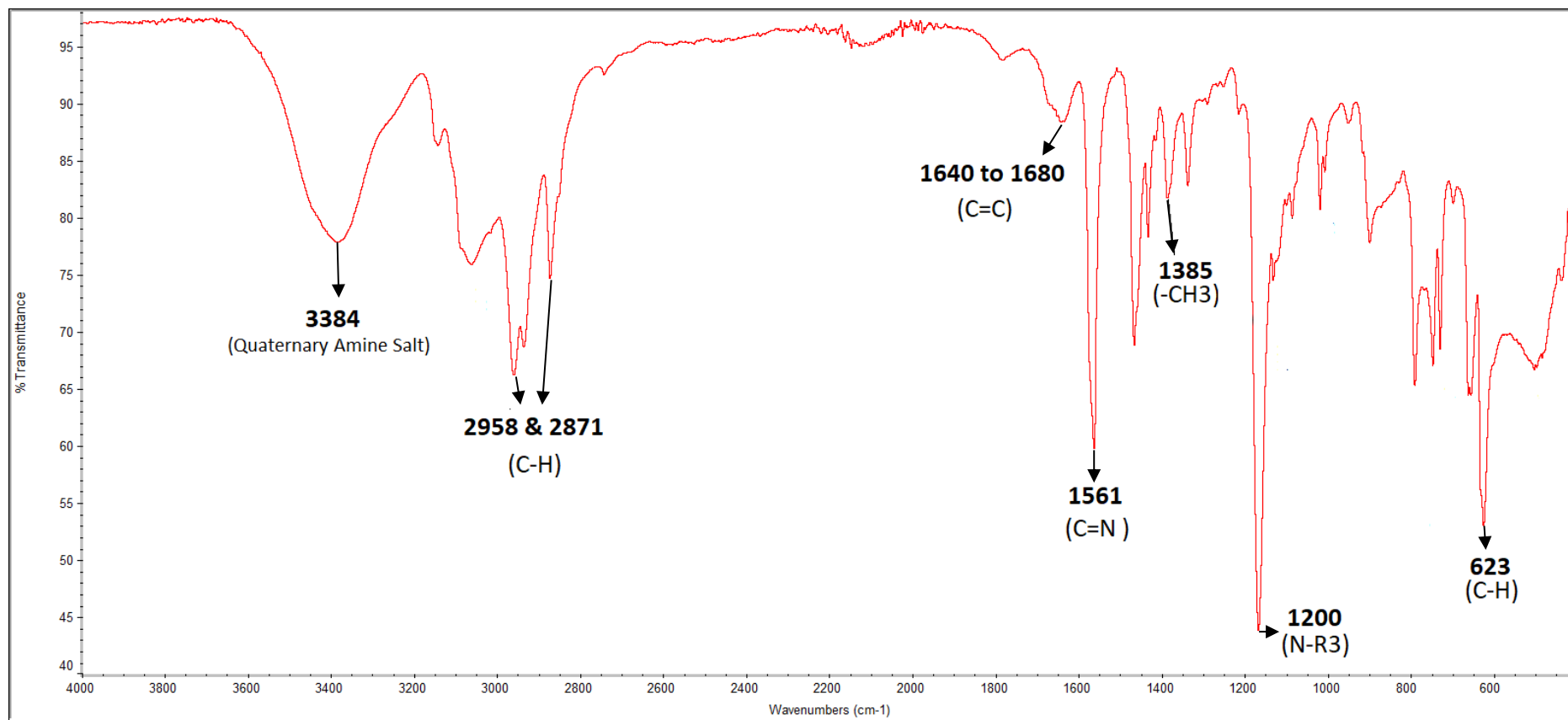


Figure 4.1: FTIR Spectra of [BMIM]Cl.

4.2.2 UV-Vis Analysis

UV-Vis analysis was conducted to characterise [BMIM]Cl. The results indicated the presence of a single strong absorption peak at 227 nm and the absorption decreased along with longer wavelength. Figure 4.2 showed that there was only one chromophore contained in the sample (Pratiwi, et al., 2022). The wavelength of the maximum absorption peak was similar to the result reported by Khalili Dermami, et al. (2019) and Danielewicz, et al. (2019), which were 207 nm and 235 nm respectively for the [BMIM]Cl sample. According to Khalili Dermami, et al. (2019), the absorption peak ranging from 190 to 260 nm was attributed to the butyl-methylimidazolium residue. The research of Shiflett (2007) also stated that the absorption peak at 210 nm was due to the π - π^* transition contributing from the C=C of the imidazolium ring. Hence, it can be concluded that the sample contained an imidazolium ring and was identified as [BMIM]Cl.

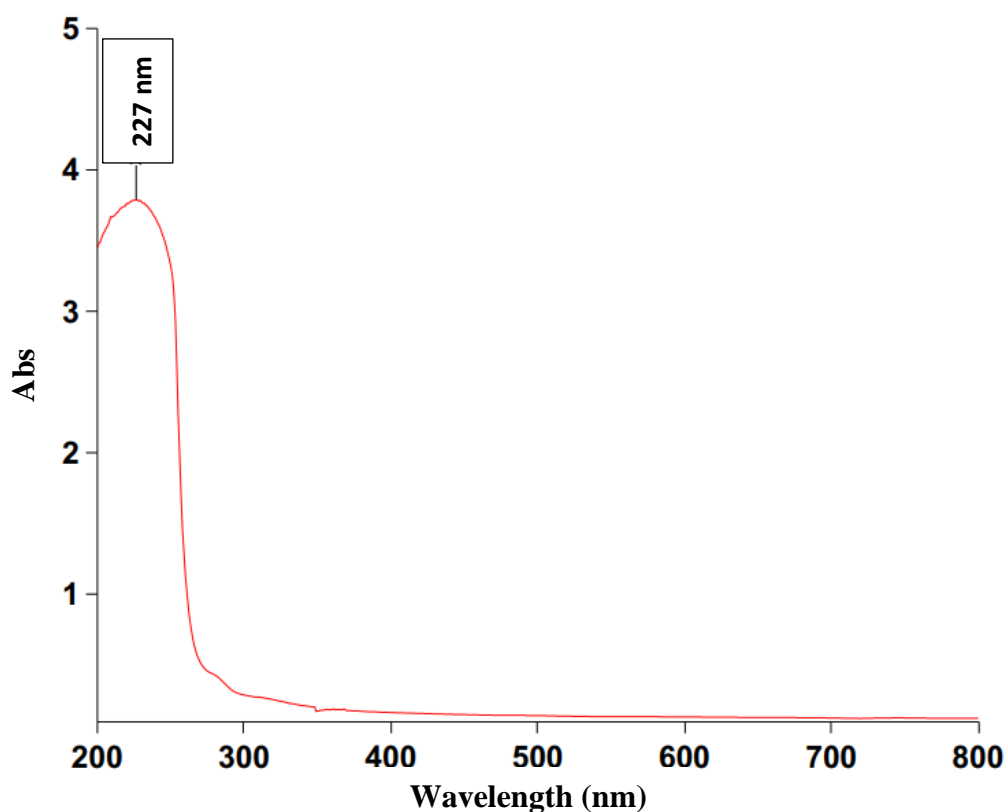


Figure 4.2: UV-Vis Spectrum of [BMIM]Cl.

4.2.3 TGA Analysis

The thermal stabilities of [BMIM]Cl were investigated using TGA. As shown in Figure 4.3, [BMIM]Cl had a single decomposition peak with a significant weight loss occurring at around 240 °C and ending around 320 °C. The weight loss was attributed to the decomposition of [BMIM]Cl molecules (Kassaye, et al., 2016). No further decomposition was observed after the decomposition of [BMIM]Cl. The result showed that [BMIM]Cl exhibited a high thermal stability up to a temperature range of 320 – 350 °C. The thermal stability information is important for identifying the temperature limit of [BMIM]Cl, which is vital in designing and optimizing esterification reaction of PFAD in the presence of [BMIM]Cl.

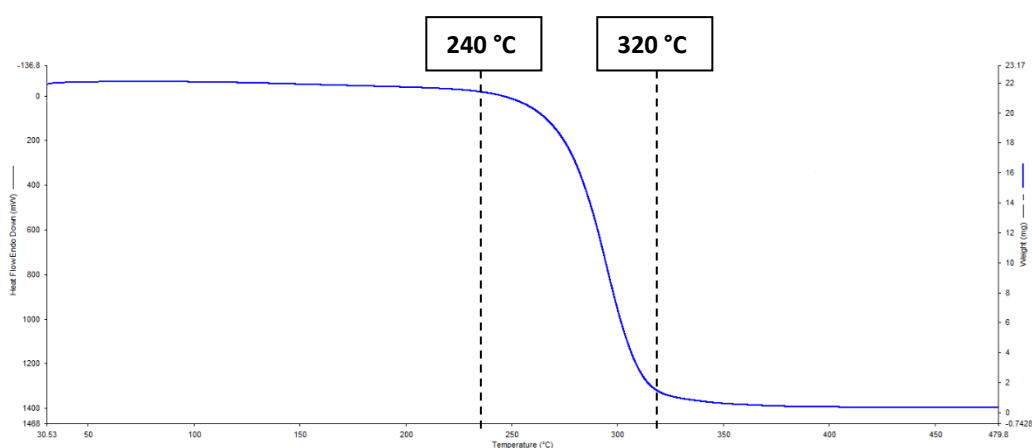


Figure 4.3: TGA Curve for [BMIM]Cl.

4.3 Parameter Study for the Esterification of Palm Fatty Acid Distillate Using 1-Butyl-3-Methylimidazolium as Catalyst

The study investigated the impact of process parameters such as temperature, catalyst dosage, methanol to PFAD ratio, and reaction time on PFAD conversion during esterification with [BMIM]Cl as a catalyst. The parameter study was performed using the design of experiment (DOE).

4.3.1 Design of Experiment (DOE)

The DOE was performed based the following process parameters: temperature (45 - 65 °C), catalyst dosage (2 – 6 wt%), methanol to PFAD ratio (5 – 25), and reaction time (1 – 5 h), with the conversion of PFAD as the response variable. Table 4.1 presented the results of the esterification reactions carried out using different combinations of these parameters generated by the program. There were six repeated runs of experiment conducted to identify the reproducibility of the results. It was observed that the conversion of PFAD ranging from 31.55 % to 40.19 %.

Table 4.1: Various Combinations of Process Parameter and Conversion.

Run	A: Temperatur e (°C)	B: Catalyst dosage (wt%)	C: Methanol to PFAD ratio	D: Reaction Time (h)	Conversion (%)
1	55	4	25	3	34.47
2	55	4	15	3	33.85
3	50	5	10	4	35.13
4	55	6	15	3	39.70
5	50	5	20	2	35.23
6	50	3	10	2	32.36
7	50	3	20	4	33.24
8	55	4	15	1	32.36
9	55	4	15	5	35.73
10	55	2	15	3	32.08
11	60	5	10	2	36.82
12	50	5	10	2	32.95
13	55	4	15	3	34.97
14	65	4	15	3	40.00
15	50	3	10	4	31.76
16	55	4	15	3	34.70
17	60	3	20	2	33.95
18	60	3	10	2	33.82
19	55	4	5	3	35.47

20	55	4	15	3	34.56
21	50	3	20	2	32.47
22	60	3	20	4	35.67
23	60	5	10	4	39.40
24	60	5	20	2	38.12
25	45	4	15	3	31.55
26	55	4	15	3	33.25
27	60	5	20	4	40.19
28	60	3	10	4	36.72
29	55	4	15	3	34.98
30	50	5	20	4	37.17

4.3.2 Statistical Analysis of Results

The results of experiments were analysed using DOE and multiple regression analysis was used to identify a suitable polynomial model to represent the data. A linear and quadratic model were suggested, and the quadratic model was chosen. The ANOVA statistical analysis at a 95% confidence interval was used to determine the effect of process parameters on the conversion of PFAD. Table 4.2 presented the statistical analysis of ANOVA.

The Fisher-test (F-test) was applied to verify the suitability of the selected model and the significance of process parameters in affecting the conversion of PFAD. The calculated F-value for quadratic model was 19.64, which indicated that the model fitted the real reaction process well and all process parameters were significant to the conversion of PFAD at 95 % CI. Additionally, the lack of fit F-value of 1.45 showed that the quadratic model fitted the data well. However, a p-value of 0.3572 implied that there was a 35.72 % chance that the lack of fit F-value could be caused by noise. This could be caused by factors such as nonlinearity of data and a higher-order polynomial model such as cubic, should be considered. However, the regression analysis predicted that the cubic model not suitable, so the quadratic model was selected. The significant parameters were determined by the p-values of the process parameters, and only the model term of A (temperature), B (catalyst dosage), D (reaction time), A^2 , and B^2 were significant as their p-values were less than 0.05. The p-values of model term C (methanol to PFAD ratio), AB, AC, AD, BC, BD,

CD, C², and D² were greater than 0.1, which implied that the parameters were not significant to the conversion of PFAD.

Table 4.2: ANOVA result of Response Surface Model for Esterification of PFAD using [BMIM]Cl as Catalyst.

Sources	Sum of Squares	df	Mean Square	F-value	p-value
Model	171.68	14	12.26	19.64	< 0.0001*
A - Temperature	70.93	1	70.93	113.61	< 0.0001*
B - Catalyst	67.54	1	67.54	108.17	< 0.0001*
C - MeOH/PFAD ratio	1.08	1	1.08	1.72	0.2091
D - Time	17.17	1	17.17	27.5	< 0.0001*
AB	0.8649	1	0.8649	1.39	0.2575
AC	1.4	1	1.4	2.25	0.1544
AD	1.55	1	1.55	2.48	0.136
BC	2.06	1	2.06	3.3	0.0894
BD	0.99	1	0.99	1.59	0.2272
CD	0.0196	1	0.0196	0.0314	0.8617
A ²	3.76	1	3.76	6.02	0.0268 *
B ²	4.39	1	4.39	7.04	0.0181*
C ²	0.7946	1	0.7946	1.27	0.277
D ²	0.1022	1	0.1022	0.1637	0.6915
Residual	9.37	15	0.6243		
Lack of Fit	6.96	10	0.6965	1.45	0.3572
Pure Error	2.4	5	0.4801		
Cor Total	181.05	29			

R² = 0.9483; Adjusted R² = 0.9000; Predicted R² = 0.7593; Adeq Precision = 15.9442; Standard Deviation = 07902; Mean = 35.09.

Note: * Significant at 95 % confident level

4.3.3 Development of Regression Model Equation

The regression analysis established a quadratic model equation in coded factor that demonstrated the relationship between the conversion of PFAD and process parameters as shown in Equation 4.1. The equation indicated that the process parameters A, B, D, A², and B² had a positive effect on the conversion of PFAD, implying that increasing these parameters could improve the conversion of PFAD.

$$\text{Conversion (\%)} = 34.39 + 1.72A + 1.68B + 0.8458D + 0.3702A^2 + 0.4002B^2 \quad (4.1)$$

where,

A = Temperature (°C)

B = Catalyst dosage (wt%)

D = Reaction time (h)

A² = Quadratic function of temperature

B² = Quadratic function of catalysts dosage

Figure 4.4 illustrated the plot of predicted and actual conversion of PFAD using the developed quadratic model equation. The ANOVA result in Table 4.2, indicated that the predicted R² and adjusted R² were 0.9 and 0.7593, respectively, with a difference less than 0.2. The adequate precision value of 15.9442 was greater than 4, indicating that the quadratic model could be applied to explore the design space. Moreover, the R² value of 0.9483 was almost equal to unity, indicating that about 95% of the total variation in the response was explained by the model. Thus, the generated model equation accurately represented the relationship between the process parameter and the conversion of PFAD.

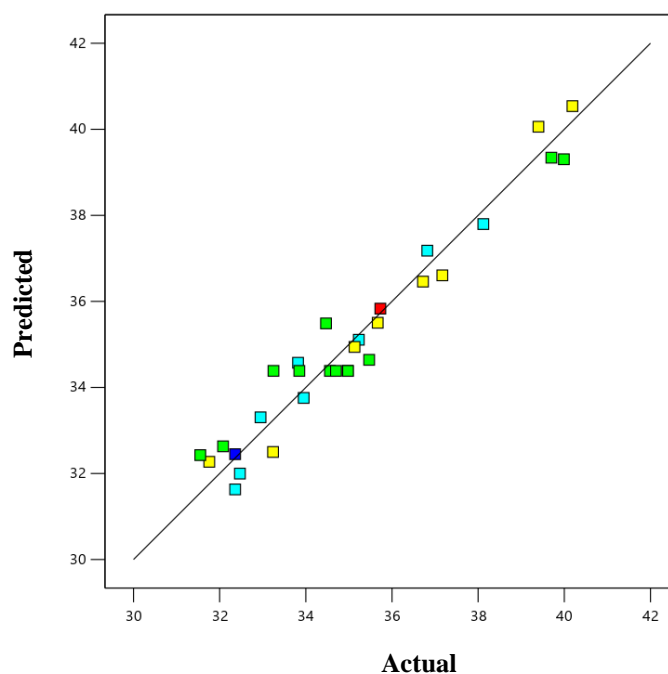


Figure 4.4: Graph of Predicted versus Actual Values of PFAD Conversion ($R^2=0.9483$).

4.3.4 Effect of Process Parameters on Esterification of Palm Fatty Acid Distillate Using 1-Butyl-3-Methylimidazolium as Catalyst

The conversion of PFAD was found to be affected by significant parameters, namely temperature (A), catalyst dosage (B), and reaction time (D) and the corresponding high order term (A^2 and B^2). According to Roman, et al. (2019), the parameters with the largest F-value indicated that the process parameter with the greatest effect on the conversion of PFAD. Based on Table 4.2, the most significant parameters affecting the conversion of PFAD in descending order were temperature (A), catalyst dosage (B), reaction time (D), higher order of catalyst (B^2) and higher order of temperature (A^2). It was interesting to highlight that the methanol to PFAD ratio (C) was found to be insignificant to the conversion of PFAD. The effect of individual process parameters including temperature, catalyst dosage, methanol-to-PFAD ratio, and reaction time, will be further discussed in the subsequent section.

i) **Effect of Temperature**

The effect of temperature on PFAD conversion was analyzed and presented in Figure 4.5. The results demonstrated that increasing the reaction temperature had a positive effect on the conversion of PFAD. As highlighted in Section 4.2 ANOVA analysis, the reaction temperature had the most significant impact to the conversion of PFAD. This could be attributed to the reduction in the viscosity of PFAD at higher temperatures, which could increase the contact between the methanol and PFAD, ultimately increasing the reaction rate (Ullah, et al., 2017). The increased in temperature also enhanced the mass transfer rates of the reactant molecules by providing the reactant molecules with more kinetic energy, resulting in an increased collision rate and consequently, a shorter reaction time (Mohammad Fauzi and Saidina Amin, 2013). These outcomes were similar to the findings of Mohammad Fauzi and Saidina Amin (2013) in which the reaction temperature was the most significant parameter for the esterification of oleic acid using [BMIM][CH₃SO₃].

Additionally, the research conducted by Guo, et al. (2011) reported that the temperature was the most significant factor in the conversion rate, recommending a high temperature ranging from 80 - 140°C to promote the conversion rate due to the low activity of ionic liquids. A similar finding was reported by Man, et al. (2013) where temperature was identified as the significant variable to achieve a higher conversion rate in esterification of crude palm oil using triethylammonium hydrogen sulfate [Et₃N][HSO₄] as the catalyst. The study from Man, et al. (2013) showed that increasing the temperature from 120 °C to 180 °C resulted in an increase in conversion rate from 20 % to 85 %. In this study, the reaction was limited to low temperature ranging from 45 – 65 °C to synthesis biodiesel through esterification reaction using [BMIM]Cl as catalyst. This limitation was due to reflux system used, which made the system impossible to reach temperatures higher than the boiling point of methanol (65 °C). Figure 4.5 also showed that the conversion of PFAD increased exponentially with increasing reaction temperature, indicating that higher temperature improved the conversion rate. Hence, low temperature could be the main factor contributing to the low conversion of PFAD in this study.

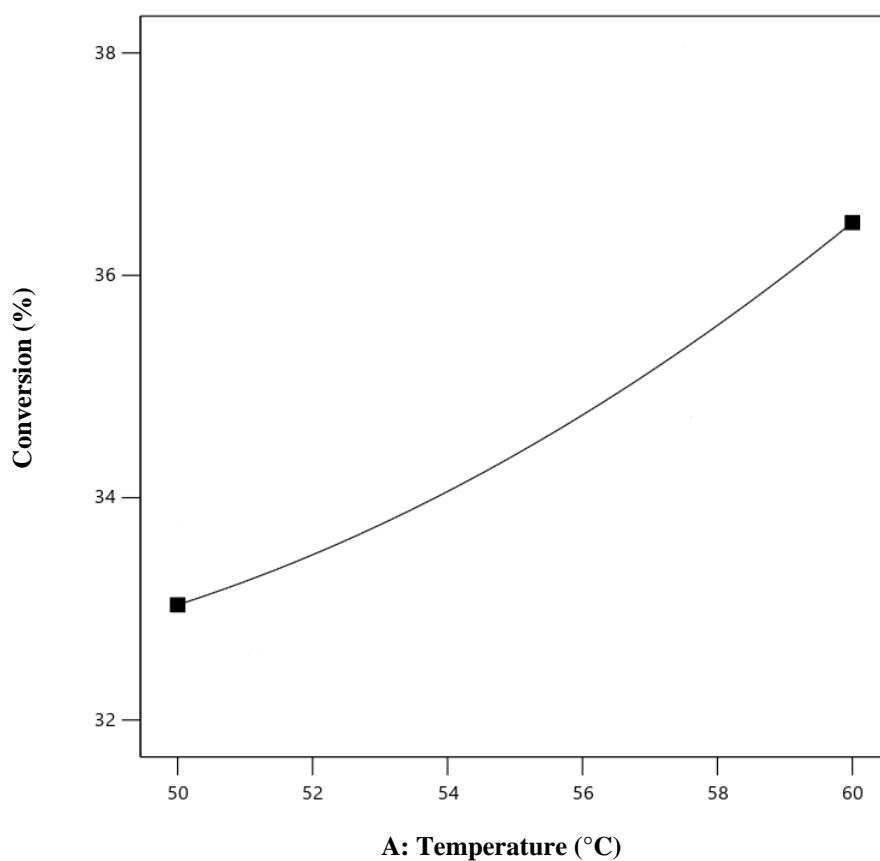


Figure 4.5: Effect of temperature to conversion of PFAD (catalyst dosage = 4 wt%, methanol to PFAD ratio = 15, reaction time = 3 h).

ii) Effect of Catalyst Dosage

The impact of catalyst dosage on the conversion of PFAD was presented in Figure 4.6. It could be observed that the conversion rate increased exponentially with the catalyst dosage. The same trend was also observed in the study by Ullah, et al. (2017), where the conversion rate was found to increase with the increase in catalyst concentration and the highest conversion was attained at a catalyst concentration of 5 wt%. This was due to the increased number of active sites available for catalyzing the reaction due to the increased catalyst concentration, leading to the enhancement of the conversion rate (Sangar, et al., 2019; Chabukswar, et al., 2013).

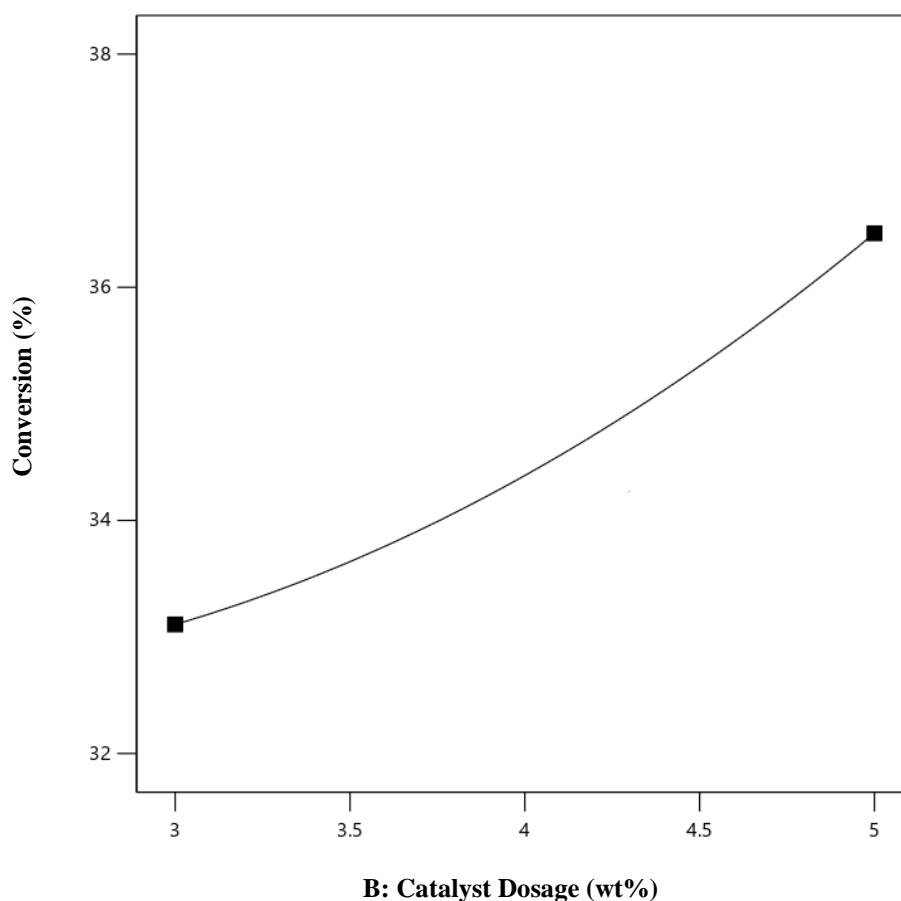


Figure 4.6: Effect of catalyst dosage to conversion of PFAD (temperature = 55 °C, methanol to PFAD ratio = 15, reaction time = 3 h).

iii) Effect of Methanol to PFAD Ratio

The effect of methanol to PFAD ratio on the PFAD was presented in Figure 4.7. It was interesting to note that the ratio had no significant effect on the conversion rate. However, previous research conducted by Sangar, et al. (2019) showed that the conversion of FFAs increased with methanol to PFAD ratio due to the excess amount of methanol that shifted the reversible reaction towards the products' side. The research also reported that further increment of methanol to PFAD ratio did not enhance the conversion rate due to excessive amount of methanol could cause active sites of the catalyst to be flooded with methanol molecules rather than PFAD molecules, reducing the conversion rate (Hindryawati, et al., 2020). Sangar, et al. (2019) also stated that the excessive methanol may increase water content in the system, pushing the reaction backward and diluting the reaction system, leading to a slower reaction and reduced conversion rate (Sangar, et al., 2019). Similar findings were observed by Ullah, et al. (2017),

where the optimum methanol to oil ratio was 12:1 and further increments of methanol amount will not have significant effect to the product yield. Hence, the insignificant effect of methanol to PFAD ratio in this study may be due to a low ratio was sufficient to drive the esterification reaction to products' side. However, increasing the methanol to PFAD ratio would still slightly increased the conversion rate by reducing the viscosity of reaction media and improving the contact between the two phase (Ullah, et al., 2017). The insignificant effect of methanol to PFAD ratio could be one of the advantage in the biodiesel production as low consumption of methanol reduces the production cost.

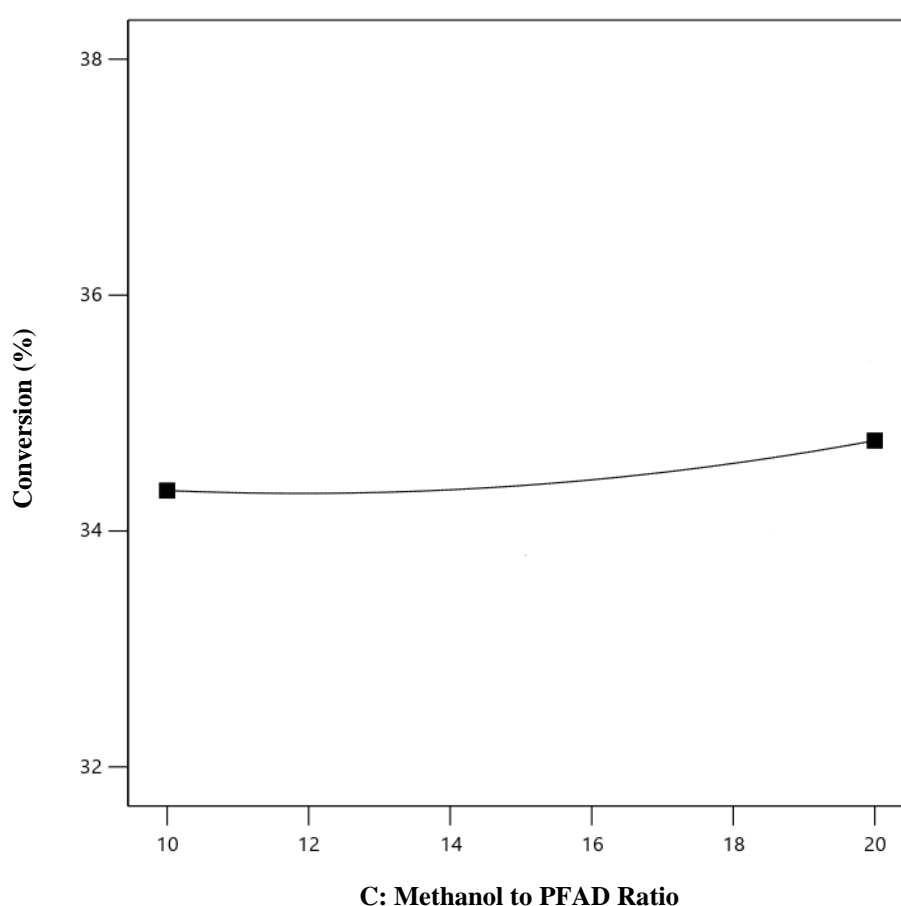


Figure 4.7: Effect of to methanol to PFAD ratio conversion of PFAD (temperature = 55 °C, catalyst dosage = 4 wt%, reaction time = 3h).

iv) Effect of Reaction Time

Figure 4.8 illustrated the impact of reaction time on the conversion of PFAD, where it was observed that the conversion rate increased linearly with the reaction time. This finding was consistent with the results reported by Guo, et al. (2011) who conducted a study on the esterification reaction of oleic acid using ionic liquid [BMIM][CH₃SO₃]-AlCl₃ as catalyst and found that a longer reaction time resulted in a higher conversion rate. They obtained nearly complete conversion after 5 hours of reaction time. This was due to the reaction required sufficient time to mix the PFAD, methanol and [BMIM]Cl phases (Ullah, et al., 2017). Hence, a longer reaction time facilitated the mixing of the three phases and minimized mass transfer between PFAD-methanol-[BMIM]Cl. Therefore, the conversion rate was enhanced with the increase in reaction time.

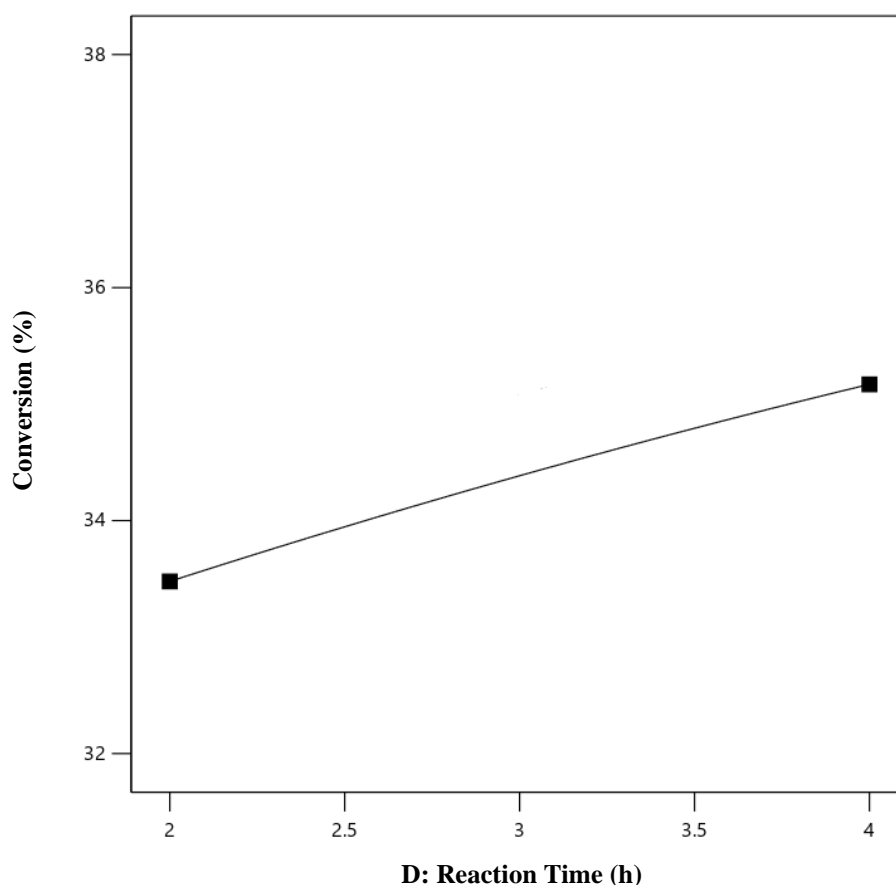


Figure 4.8: Effect of reaction time to conversion of PFAD (temperature = 55 °C, catalyst dosage = 4 wt%, methanol to PFAD ratio = 3h).

4.4 GC Analysis

GC analysis was employed to characterize sample of biodiesel and PFAD. GC analysis aided in determining whether the esterification of PFAD using [BMIM]Cl as catalyst had converted the FFAs into methyl ester or biodiesel. Figure 4.9 and Figure 4.10 showed the GC spectrum of pure PFAD and biodiesel sample, respectively. The research study from Shuit (2015) discovered that PFAD contained various FFAs included myristic acid (C14:0), palmitic acid (C16:0), stearic acid (C18:0), oleic acid (C18:1), and linoleic acid (C18:2). Based on the GC analysis, the biodiesel sample had five similar peaks to the spectrum of PFAD at a retention time of 19.719, 27.402, 40.667, and 43.310 min, which could be contributed to the FFAs in PFAD, indicating the presence of unconverted PFAD in the sample. On the other hand, the peaks at retention time of 12.089 and 14.836 min attributed to methyl palmitate and methyl stearate, respectively (David, et al., 2014). Table 4.3 and Table 4.4 summarised the identification of peaks in GC spectrum of PFAD and biodiesel, respectively.

Table 4.3: Identification of Peaks in GC Spectrum of Pure PFAD.

Retention time (min)	Type of FFAs
19.750	Myristic Acid (C14:0)
27.563	Palmitic Acid (C16:0)
40.765	Stearic Acid (C18:0)
43.553	Oleic Acid (C18:1)
48.463	Linoleic Acid (C18:2)

Table 4.4: Identification of Peaks in GC Spectrum of Biodiesel Sample.

Retention time (min)	Type of Methyl Ester
12.089	Methyl Palmitate
14.836	Methyl Stearate
19.719	Myristic Acid (C14:0)
27.402	Palmitic Acid (C16:0)
40.667	Stearic Acid (C18:0)
43.310	Oleic Acid (C18:1)
48.348	Linoleic Acid (C18:2)

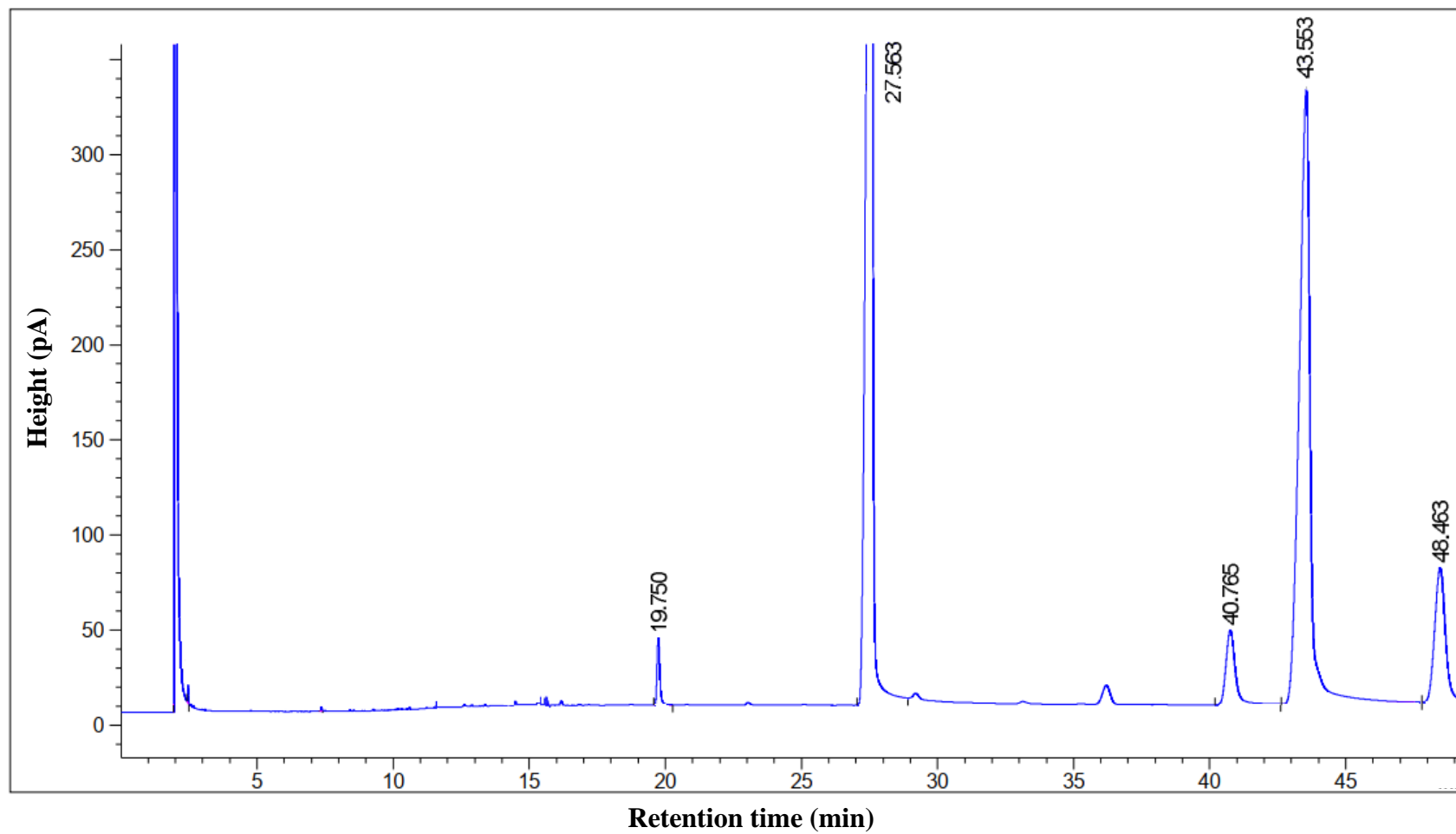


Figure 4.9: GC Spectrum of Pure PFAD.

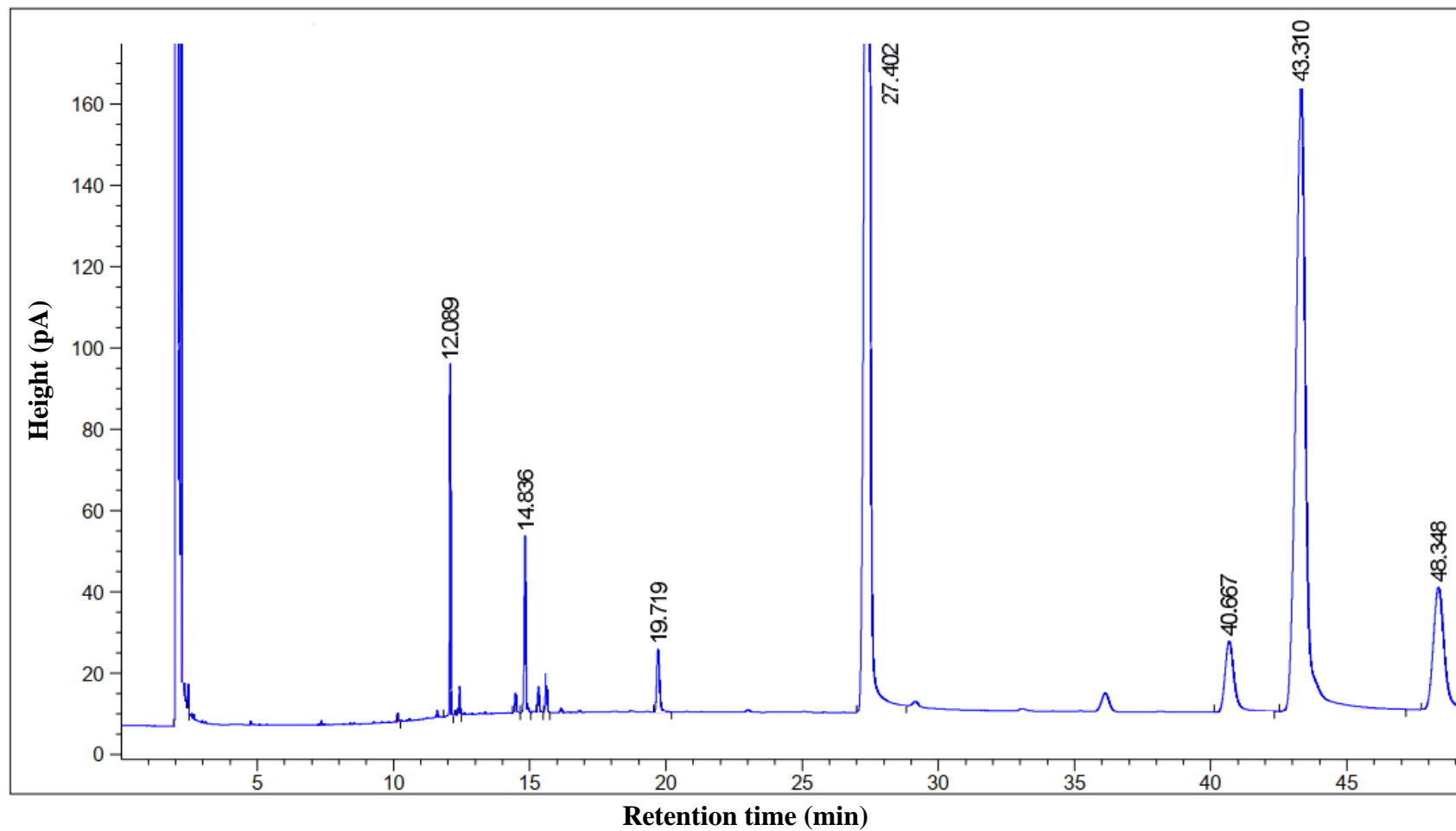


Figure 4.10: GC Spectrum of Biodiesel Sample (temperature = 65 °C, catalyst dosage = 4 wt%, methanol to PFAD ratio = 10, reaction time = 4h).

4.5 Process Optimization Studies

Process optimization plays an important role in determining the optimum parameters required for achieving highest conversion rate of PFAD. Among the several factors that affect the conversion rate, the reaction temperature was found to be the most significant. Hence, it is important to identify the optimum temperature for obtaining the maximum conversion of PFAD. Moreover, the catalyst dosage and methanol to PFAD ratio also need to be optimized so that the waste of catalyst and reactants can be minimized. Additionally, optimizing the reaction time can help in reducing the operating cost for biodiesel production. The Design Expert software's optimisation tool was used to anticipate the optimum process parameters. Table 4.5 illustrated the constraints used for optimizing the parameters.

Table 4.5: Constraints for Optimization of PFAD Conversion.

Parameters	Goal	Lower Limit	Upper Limit
A: Temperature (°C)	Is in range	50	60
B: Catalyst dosage (wt%)	Is in range	3	5
C: MeOH/PFAD ratio	Is in range	10	20
D: Time (h)	Is in range	2	4
Conversion of PFAD (%)	Maximize	31.55	40.19

According to the solution of numerical optimization using Equation 4.1, the optimal conditions for obtaining 40.24% of PFAD were identified as follows: a temperature of 60°C, a catalyst dosage of 5 wt%, a methanol to PFAD ratio of 19.6, and a reaction time of 4 hours. The optimum process conditions was verified by conducting experimental work using the recommended conditions. Table 4.6 showed the optimum conditions, the predicted conversion generated by the program, the experimental result, and the percentage error of the predicted result. The percentage error was calculated using Equation 4.2.

Percentage error (%)

$$= \left[\frac{PFAD\ Conversion_{experimental} - PFAD\ Conversion_{predicted}}{PFAD\ Conversion_{experimental}} \right] \times 100\% \quad (4.2)$$

Table 4.6: Model Validation Conducted at Optimum Condition.

Variable	Value
A: Temperature (°C)	60
B: Catalyst dosage (wt%)	5
C: MeOH/PFAD ratio	19.6
D: Time (h)	4
Predicted conversion of PFAD (%)	40.27
Experimental conversion of PFAD (%)	38.44
Percentage error (%)	4.76

4.6 Summary

In summary, the ANOVA analysis as shown in Table 4.2 showed that the process parameters such as temperature (A), catalyst dosage (B), reaction time (D), quadratic function of temperature (A^2), and quadratic function of catalyst dosage (B^2), had significant effects on the conversion PFAD. Among these parameters, temperature had the most significant effect on the conversion rate, with an F-value of 113.61. Based on the quadratic model equation as shown in Equation 4.1, a predicted versus actual PFAD conversion graph was plotted, and an R^2 value of 0.9483 was obtained. Furthermore, it was found that the methanol to PFAD ratio had an insignificant effect on the conversion rate, meaning the reaction could be driven to the product side with a low amount of methanol. The process parameters were then optimized using Design Expert 13. The optimized conditions were identified as follows: temperature of 60 °C, catalyst dosage of 4.97%, methanol to PFAD ratio of 19.6, and a reaction time of 4 hours. These conditions yielded an optimal conversion rate of 40.24%. The optimum conditions were verified experimentally and obtained a percentage error of 4.87 %. Additionally, it was observed that low reaction temperature (below 65 °C) could be the main factor that cause a low conversion in PFAD (31.55 to 40.19 %).

CHAPTER 5

CONCLUSIONS AND RECOMMENDATIONS

5.1 Conclusions

Biodiesel was successfully synthesized through esterification of PFAD using [BMIM]Cl as catalyst. The characterization of [BMIM]Cl was done before conducting the experimental work using FTIR, UV-Vis, and TGA. FTIR result showed the presence of several function groups in [BMIM]Cl sample, including quaternary amine salt formation with chlorine, C-H, C=N, C=C, -CH₃. Besides, [BMIM]Cl also showed a strong absorption peak at 227 nm in the UV-Vis analysis, indicating the presence of C=C in the imidazolium ring. Moreover, the TGA analysis showed a single decomposition peak was occurred at temperature ranging from 240 to 320 °C, indicating a high thermal stability for [BMIM]Cl.

The PFAD conversion was investigated by applying response surface methodology (RSM) coupled with centre composite design (CCD) model using Design Expert software to investigate the impact of process parameters, which were temperature (45 – 65 °C), catalyst dosage (2 – 6 wt%), methanol to PFAD ratio (5 – 25), and reaction time (1 – 5 h). The optimal conditions for achieving the maximum conversion of 40.24% of PFAD, which were determined to be a temperature of 60°C, a catalyst dosage of 5 wt%, a methanol to PFAD ratio of 19.6, and a reaction time of 4 hours. Besides, the study also observed that the conversion rate was not significantly affected by methanol to PFAD ratio. This could be due to low ratio of methanol to PFAD was enough to drive the reversible reaction towards products' side. Furthermore, the low conversion of PFAD was due to the low temperature of reaction as the esterification reaction is an endothermic reaction that requires heat energy to increase the conversion rate.

5.2 Recommendations for future work

This study has shown the feasibility of ionic liquid [BMIM]Cl in producing biodiesel through esterification of PFAD with methanol. Below listed the recommendations for further improving this research project in the future:

1. This present study had showed a low conversion rate of PFAD under low temperature (below 65 °C). This project can be further studied using autoclave sealed type reactor rather than reflux system. Most of the research on the biodiesel production using ionic liquid was conducted at high temperature since the endothermic reaction required heat to provide kinetic energy to the reactant molecules and therefore enhanced the conversion rate. By replacing the reflux system with autoclave type sealed reactor, the system can achieve higher temperature to investigate the optimum temperature for this project.
2. There is limited research conducted on the esterification of PFAD utilizing the ionic liquid [BMIM]Cl and no related research has been done on large scale production. Consequently, the upscaling of this synthesis method for industrial implementation is challenging. Hence, it is important to investigate this synthesis approach using a large scale reactor system for future commercialization in the future.

REFERENCES

- Alimova, I., Ribeiro, A. and Queiroz, A., 2017. Study of biodiesel production through esterification catalyzed by imidazolium ILs. *III Congresso Ibero-Americano de Ambiente e Tecnologia*, pp.103–107.
- Andreani, L. and Rocha, J.D., 2012. Use of ionic liquids in biodiesel production: A review. *Brazilian Journal of Chemical Engineering*, 29(1), pp.1–13.
- Anguebes-Franceschi, F. et al., 2019. Physical and chemical properties of biodiesel obtained from amazon sailfin catfish (*Pterygoplichthys pardalis*) Biomass Oil. *Journal of Chemistry*, 2019.
- Budiman, A., Lelyana, A., Rianawati, D. and Sutijan, S., 2018. Biodiesel production from palm fatty acid distillate (PFAD) using reactive distillation. *Jurnal Teknik Kimia Indonesia*, 11(2), p.108.
- Chabukswar, D.D., Heer, P.K.K.S. and Gaikar, V.G., 2013. Esterification of palm fatty acid distillate using heterogeneous sulfonated microcrystalline cellulose catalyst and its comparison with H₂SO₄ catalyzed reaction. *Industrial and Engineering Chemistry Research*, 52(22), pp.7316–7326.
- Chemistry LibreTexts., 2014. *Infrared spectroscopy absorption table*. [online] Available at: <https://chem.libretexts.org/Ancillary_Materials/Reference/Reference_Tables/Spectroscopic_Reference_Tables/Infrared_Spectroscopy_Absorption_Table> [Access 29 April 2023].
- Chemistry LibreTexts., 2015. *24.10: Spectroscopy of amines*. [online] Available at: <[https://chem.libretexts.org/Bookshelves/Organic_Chemistry/Organic_Chemistry_\(Morsch_et_al.\)/24%3A_Amines_and_Heterocycles/24.10%3A_Spectroscopy_of_Amines](https://chem.libretexts.org/Bookshelves/Organic_Chemistry/Organic_Chemistry_(Morsch_et_al.)/24%3A_Amines_and_Heterocycles/24.10%3A_Spectroscopy_of_Amines)> [Access 29 April 2023].
- Danielewicz, D., Kmiołek, M. and Surma-ślusarska, B., 2019. Study of ionic liquids UV-VIS and FTIR spectra before and after heating and spruce groundwood dissolution. *Fibres and Textiles in Eastern Europe*, 27(1), pp.118–123.
- David, F., Sandra, P. and Vickers, A.K., 2014. *Column selection for the analysis of fatty acid methyl esters application lipid changes in dry-cured ham view project micro-gc view project column selection for the analysis of fatty acid methyl esters application*.
- Demirbas, A., 2007. Importance of biodiesel as transportation fuel. *Energy Policy*, 35(9), pp.4661–4670.
- Enerdata, 2021. *Biofuel evolution perspectives*.

Figueredo, I.D.M., Rios, M.A.D.S., Cavalcante, C.L. and Luna, F.M.T., 2020. Effects of amine and phenolic based antioxidants on the stability of babassu biodiesel using rancimat and differential scanning calorimetry techniques. *Industrial and Engineering Chemistry Research*, 59(1), pp.18–24.

Fontana, F., 2018. *Biodiesel production through esterification applying ionic liquids as catalysts*.

Fukuda, H., Kondo, A. and Noda, H., 2001. Biodiesel fuel production by transesterification of oils. *Journal of Bioscience and Bioengineering*, 92(5), pp.405–416.

Gebremariam, S.N. and Marchetti, J.M., 2017. Biodiesel production technologies: Review. *AIMS Energy*, 5(3), pp.425–457.

Gholami, A., Pourfayaz, F. and Maleki, A., 2020. Recent advances of biodiesel production using ionic liquids supported on nanoporous materials as catalysts: A review. *Frontiers in Energy Research*, 8.

Gouveia, L. et al., 2017. Biodiesel from microalgae. In: *Microalgae-Based Biofuels and Bioproducts: From Feedstock Cultivation to End-Products*. Elsevier Inc., pp. 235–258.

Guo, F. et al., 2011. One-step production of biodiesel from jatropha oil with high-acid value in ionic liquids. *Bioresource Technology*, 102(11), pp.6469–6472.

Harjanne, A. and Korhonen, J.M., 2019. Abandoning the concept of renewable energy. *Energy Policy*, 127, pp.330–340.

Hindryawati, N. et al., 2020. Biodiesel production using palm fatty acid distillate and rice husk silica supported NiSO₄ as catalyst. *AIP Conference Proceedings*. American Institute of Physics Inc.

IEA, 2019. *Bioenergy - Fuels & Technologies*. [online] IEA. Available at: <<https://www.iea.org/fuels-and-technologies/bioenergy>> [Accessed 1 May 2023].

International Energy Agency, 2021. *Statistics report key world energy statistics 2021*.

Ita, B., Magu, T.O. and Ehi-Eromosele, C.O., 2018. *Physico-chemical properties of biodiesel obtained from jatropha curcas seeds oil using CoMgFe₂O₄ and MgFe₂O₄ as nanocatalysts*.

Kassaye, S., Pant, K.K. and Jain, S., 2016. Synergistic effect of ionic liquid and dilute sulphuric acid in the hydrolysis of microcrystalline cellulose. *Fuel Processing Technology*, 148, pp.289–294.

- Kaur, T. and Patyar, P., 2023. Impact of BmimCl on the thermophysical and FTIR properties of protein model compounds in aqueous solutions. *Journal of Molecular Liquids*, 369.
- Khalili Dermani, A., Kowsari, E., Ramezanzadeh, B. and Amini, R., 2019. Utilizing imidazole based ionic liquid as an environmentally friendly process for enhancement of the epoxy coating/graphene oxide composite corrosion resistance. *Journal of Industrial and Engineering Chemistry*, 79, pp.353–363.
- Khan, Z. et al., 2021. Current developments in esterification reaction: A review on process and parameters. *Journal of Industrial and Engineering Chemistry*, 103, pp.80–101.
- Koh, M.Y. and Tinia, T.I., 2011. A review of biodiesel production from *Jatropha curcas* L. oil. *Renewable and Sustainable Energy Reviews*, 15(5), pp.2240–2251.
- Latchubugata, C.S. et al., 2018. Kinetics and optimization studies using Response Surface Methodology in biodiesel production using heterogeneous catalyst. *Chemical Engineering Research and Design*, 135, pp.129–139.
- Lei, Z., Chen, B., Koo, Y.M. and Macfarlane, D.R., 2017. Introduction: Ionic Liquids. *Chemical Reviews*, 117(10), pp.6633–6635.
- Liu, C.Z., Wang, F., Stiles, A.R. and Guo, C., 2012. Ionic liquids for biofuel production: Opportunities and challenges. *Applied Energy*, 92, pp.406–414.
- Man, Z. et al., 2013. A Brønsted ammonium ionic liquid-KOH two-stage catalyst for biodiesel synthesis from crude palm oil. *Industrial Crops and Products*, 41(1), pp.144–149.
- Mandari, V. and Devarai, S.K., 2022. Biodiesel production using homogeneous, heterogeneous, and enzyme catalysts via transesterification and esterification reactions: A critical review. *Bioenergy Research*, 15(2), pp.935–961.
- Mariano, A., Soares Junior, J., Pinto Mariano, A. and de Franceschi de Angelis, D., 2009. Biodegradation of biodiesel/diesel blends by candida viswanathii production of biofuel butanol from agricultural residues view project microbial lipid production view project biodegradation of biodiesel/diesel blends by candida viswanathii. *Article in African Journal Of Biotechnology*, 8(12), pp.2774–2778.
- Martins, G.I. et al., 2015. Physical and chemical properties of fish oil biodiesel produced in Brazil. *Renewable and Sustainable Energy Reviews*, 42, pp.154–157.
- Merck (n.d.). *IR spectrum table & chart*. [online] Sigmaaldrich.com. Available at: <<https://www.sigmaaldrich.com/MY/en/technical-documents/technical-article/analytical-chemistry/photometry-and-reflectometry/ir-spectrum-table>> [Access 29 April 2023].

Mohammad Fauzi, A.H. and Saidina Amin, N.A., 2013. Optimization of oleic acid esterification catalyzed by ionic liquid for green biodiesel synthesis. *Energy Conversion and Management*, 76, pp.818–827.

Ong, H.C. et al., 2021. Recent advances in biodiesel production from agricultural products and microalgae using ionic liquids: Opportunities and challenges. *Energy Conversion and Management*, 228.

Owusu, P.A. and Asumadu-Sarkodie, S., 2016. A review of renewable energy sources, sustainability issues and climate change mitigation. *Cogent Engineering*, 3(1).

Palm Fatty Acid Distillate (PFAD) in biofuels., n.d. Available at: <<https://d5i6is0eze552.cloudfront.net/documents/Annet/Palm-Fatty-Acid-Distillate-in-biofuels.-ZERO-and-Rainforest-Foundation-N.pdf?mtime=20160302113207>> [Accessed 29 April 2023].

Panchal, B. et al., 2022. The current state applications of ethyl carbonate with ionic liquid in sustainable biodiesel production: A review. *Renewable Energy*, 181, pp.341–354.

Piemonte, V., di Paola, L., Iaquaniello, G. and Prisciandaro, M., 2016. Biodiesel production from microalgae: Ionic liquid process simulation. *Journal of Cleaner Production*, 111, pp.62–68.

Pratiwi, R.A., Bayu, A. and Nandiyanto, D., 2022. How to read and interpret uv-vis spectrophotometric results in determining the structure of chemical compounds. *Indonesian Journal of Educational Research and Technology*, 2(1), pp.1–20.

Ramadhan, A., Pornwongthong, P., Rattanaporn, K. and Sriariyanun, M., 2015. A review on biodiesel synthesis using catalyzed transesterification base ionic liquids as catalyst. *Journal Science Technology MSU*, 34(4), pp.405–412.

Renewable Energy Progress Report, 2017. Available at: <https://ec.europa.eu/energy/sites/ener/files/documents/20160713%20draft_publication_REF2016_v13.pdf> [Accessed 29 April 2023].

Roman, F.F. et al., 2019. Optimization and kinetic study of biodiesel production through esterification of oleic acid applying ionic liquids as catalysts. *Fuel*, 239, pp.1231–1239.

Sagat, M. and Toncu, D.-C., 2015. Experimental analysis of water-diesel emulsified fuels. *International Journal of Energy and Power*, 4(0), p.11.

Sangar, S.K. et al., 2019. Methyl ester production from palm fatty acid distillate (PFAD) using sulfonated cow dung-derived carbon-based solid acid catalyst. *Energy Conversion and Management*, 196, pp.1306–1315.

Sani, S. et al., 2018. Determination of physico chemical properties of biodiesel from *Citrullus lanatus* seeds oil and diesel blends, *Industrial Crops and*

Products, 122, pp. 702–708. Available at: <https://doi.org/10.1016/j.indcrop.2018.06.002>.

Shiflett, M.B., Yokozeki, A., Rahman, M.A. and Yokoyama, C., 2007. Absorption spectra of imidazolium ionic liquids. *The Journal of Physical Chemistry B*, 111(33), pp.9859-9863.

Shuit, S.H., 2015. *Studies on the sulfonated carbon nanotubes catalyst and membrane reactor for biodiesel production*. [pdf] p.98. Available at: <http://eprints.usm.my/40782/1/Studies_on_the_sulfonated_carbon_nanotubes_catalyst_and_membrane_reactor_for_biodiesel_production_Shuit_Siew_Hoong_K4_2015_MJMS.pdf> [Accessed 26 April 2023].

Shuit, S.H. and Tan, S.H., 2019. Esterification of palm fatty acid distillate with methanol via single-step pervaporation membrane reactor: A novel biodiesel production method, *Energy Conversion and Management*, 201. Available at: <<https://doi.org/10.1016/j.enconman.2019.112110>> [Accessed 26 April 2023].

Suthisripok, T. and Semsamran, P., 2018. The impact of biodiesel B100 on a small agricultural diesel engine. *Tribology International*, 128, pp.397–409.

Tabatabaei, M. et al., 2019. Reactor technologies for biodiesel production and processing: A review. *Progress in Energy and Combustion Science*, 74, pp.239–303.

Troter, D.Z. et al., 2016. Application of ionic liquids and deep eutectic solvents in biodiesel production: A review. *Renewable and Sustainable Energy Reviews*, 61, pp.473–500.

Ullah, Z. et al., 2018. A review on ionic liquids as perspective catalysts in transesterification of different feedstock oil into biodiesel. *Journal of Molecular Liquids*, 266, pp.673–686.

Ullah, Z. et al., 2017. Preparation and kinetics study of biodiesel production from waste cooking oil using new functionalized ionic liquids as catalysts. *Renewable Energy*, 114, pp.755–765. Available at: <https://linkinghub.elsevier.com/retrieve/pii/S0960148117307127>.

Ullah, Z., Bustam, M.A. and Man, Z., 2015. Biodiesel production from waste cooking oil by acidic ionic liquid as a catalyst. *Renewable Energy*, 77, pp.521–526.

U.S. Energy Information Administration (EIA), 2022. *Monthly energy review – July 2002*. [pdf] Available at: < www.eia.gov/mer > [Access 26 April 2023].

Wang, S. et al., 2020. Synthesis cyclic carbonates with BmimCl-based ternary deep eutectic solvents system. *Journal of CO2 Utilization*, 40.

Win, S.S. and Trabold, T.A., 2018. Sustainable waste-to-energy technologies: transesterification. *Sustainable Food Waste-to-Energy Systems*, pp.89–109.

Wu, Q. et al., 2007. Transesterification of cottonseed oil catalyzed by brønsted acidic ionic liquids. *Industrial and Engineering Chemistry Research*, 46(24), pp.7955–7960.

Yassin, F.A. et al., 2015. Highly effective ionic liquids for biodiesel production from waste vegetable oils. *Egyptian Journal of Petroleum*, 24(1), pp.103–111.

Zeng, Z. et al., 2012. *Recent Developments on the Mechanism and Kinetics of Esterification Reaction Promoted by Various Catalysts, Chemical Kinetics*,

Zhang, X. et al., 1998. Biodegradability of biodiesel in the aquatic environment. *Trans. ASAE*, 41(5), pp.1423–1430.

APPENDICES

APPENDIX A: Preparation of 0.1 M NaOH from 97 % NaOH

The mass of NaOH pellet that was required to prepare 0.1 M of NaOH in 0.5 L solution is calculated as follows:

Number of moles of NaOH:

$$\begin{aligned}
 \text{Number of moles of NaOH(pure)} &= \text{Molarity} \times \text{Volume} \\
 &= 0.1 \frac{\text{mol}}{\text{L}} \times 0.5 \text{ L} \\
 &= 0.05 \text{ mol}
 \end{aligned}$$

Since NaOH with purity of 97 %, the number of moles of NaOH was recalculated,

$$\begin{aligned}
 0.97 \times \text{Number of moles of NaOH (97\%)} &= 0.05 \text{ mol} \\
 \text{Number of moles of NaOH (97\%)} &= \frac{0.05 \text{ mol}}{0.97} \\
 &= 0.0515 \text{ mol}
 \end{aligned}$$

Mass of NaOH pellet:

Molecular weight, MW of NaOH = 40 g/mol,

$$\begin{aligned}
 \text{Mass of NaOH} &= \text{Number of moles of NaOH} \times \text{MW of NaOH} \\
 &= 0.0515 \text{ mol} \times 40 \frac{\text{g}}{\text{mol}} \\
 &= 2.06 \text{ g}
 \end{aligned}$$

Therefore, 2.06 g of NaOH pellet was dissolved in 500 mL distilled water to prepare 0.1 M of NaOH solution.

APPENDIX B: Determination of PFAD conversion rate

The conversion rate of PFAD was calculated based on the change of acid value (AV) in the sample. The sample calculation as shown below was performed based on titration result of reaction run 1. Table B-3 summarized the calculated acid value and conversion of PFAD.

1. Initial AV:

Weight of PFAD, $m = 1$ g

Molarity of NaOH, $C = 1$ M

Molecular weight of NaOH, $MW = 40$ g/mol

Table B-1: Titration Result of Pure PFAD.

	1	2	3
Volume of NaOH used in titration, V (mL)	50.0	49.5	51.5
Average (mL)	50.0		

$$\begin{aligned}
 AV_{PFAD} &= \frac{MW_{NaOH} \times C_{NaOH} \times V_{NaOH}}{m_{PFAD}} \\
 &= \frac{40 \frac{g}{mol} \times 0.1 \frac{mol}{L} \times 50 \text{ mL}}{1 \text{ g}} \\
 &= 200.00 \text{ mgNaOH/g PFAD}
 \end{aligned}$$

2. Final AV (Run 1):

Weight of biodiesel sample (Run 1), $m = 1$ g

Molarity of NaOH, $C = 0.1$ M

Molecular weight of NaOH, $MW = 40$ g/mol

Table B-2: Titration Result of Biodiesel Sample (Run 1).

	1	2	3
Volume of NaOH used in titration, V (mL)	32.8	34.2	31.3
Average (mL)	33.765		

$$\begin{aligned}
 AV_{sample} &= \frac{MW_{NaOH} \times C_{NaOH} \times V_{NaOH}}{m_{sample}} \\
 &= \frac{40 \frac{g}{mol} \times 0.1 \frac{mol}{L} \times 33.765 mL}{1 g} \\
 &= 131.07 mgNaOH/g biodiesel
 \end{aligned}$$

3. Conversion rate of PFAD (Run 1):

$$\begin{aligned}
 Conversion (\%) &= \frac{AV_{PFAD} - AV_{sample}}{AV_{PFAD}} \times 100\% \\
 &= \frac{200.00 - 131.07}{200.00} \times 100\% \\
 &= 34.47 \%
 \end{aligned}$$

Hence, the conversion rate of PFAD for reaction run 1 is 34.47 %.

Table B-3: Summary of acid value and PFAD conversion determination.

Run	m (g)	V (mL)	C (mol/L)	AV (mg NaOH/ g biodiesel)	Conversion (%)
PFAD	1	0.500	0.1	200	-
1	1	32.765	0.1	131.06	34.47
2	1	33.075	0.1	132.30	33.85
3	1	32.435	0.1	129.74	35.13
4	1	30.150	0.1	120.60	39.7
5	1	32.385	0.1	129.54	35.23
6	1	33.820	0.1	135.28	32.36
7	1	33.380	0.1	133.52	33.24
8	1	33.820	0.1	135.28	32.36
9	1	32.135	0.1	128.54	35.73
10	1	33.960	0.1	135.84	32.08
11	1	31.590	0.1	126.36	36.82
12	1	33.525	0.1	134.10	32.95
13	1	32.515	0.1	130.06	34.97

14	1	30.000	0.1	120.00	40
15	1	34.120	0.1	136.48	31.76
16	1	32.650	0.1	130.60	34.7
17	1	33.025	0.1	132.10	33.95
18	1	33.090	0.1	132.36	33.82
19	1	32.265	0.1	129.06	35.47
20	1	32.720	0.1	130.88	34.56
21	1	33.765	0.1	135.06	32.47
22	1	32.165	0.1	128.66	35.67
23	1	30.300	0.1	121.20	39.4
24	1	30.940	0.1	123.76	38.12
25	1	34.225	0.1	136.90	31.55
26	1	33.375	0.1	133.50	33.25
27	1	29.905	0.1	119.62	40.19
28	1	31.640	0.1	126.56	36.72
29	1	32.510	0.1	130.04	34.98
30	1	31.415	0.1	125.66	37.17
